https://doi.org/10.5194/bg-2019-284
Preprint. Discussion started: 29 August 2019

Organic matter and sediment properties determine in-lake variability of sediment CO_2 and CH_4 production and emissions of a small and shallow lake

Leandra Stephanie Emilia Praetzel[1], Nora Plenter[2,3], Sabrina Schilling[1], Marcel Schmiedeskamp[1], Gabriele Broll[2], Klaus-Holger Knorr[1]

[1]University of Münster, Institute of Landscape Ecology, Biogeochemistry and Ecohydrology Research Group

[2]University of Osnabrück, Institute of Geography, Agroecology and Soil Research Group

[3]University of Applied Sciences Osnabrück, Faculty of Agricultural Sciences and Landscape Architecture

Correspondence to: Leandra S. E. Praetzel (leandra.praetzel@uni-muenster.de) or Klaus-Holger Knorr (kh.knorr@uni-muenster.de)

https://doi.org/10.5194/bg-2019-284
Preprint. Discussion started: 29 August 2019

Biogeosciences Discussions

Abstract

Inland waters are significant sources of CO_2 and CH_4 to the atmosphere, following recent studies this is particularly the case for small and shallow lakes. The spatial in-lake heterogeneity of CO_2 and CH_4 production processes and their drivers in the sediment yet remain poorly studied. We thus measured potential CO_2 and CH_4 production in sediment incubations from 12 sites within the small and shallow crater lake Windsborn in Germany as well as fluxes at the water-atmosphere interface at four sites. Production rates were highly variable and ranged from 7.2 and 38.5 µmol CO_2 gC^{-1} d^{-1} and from 5.4 to 33.5 µmol CH_4 gC^{-1} d^{-1}. Fluxes lay between 4.5 and 26.9 mmol CO_2 m^{-2} d^{-1} and between 0 and 9.8 mmol CH_4 m^{-2} d^{-1}. Both CO_2 and CH_4 production rates and CH_4 fluxes were significantly negative ($p<0.05$, rho<-0.6) correlated with the prevalence of recalcitrant organic matter compounds in the sediment as identified by FTIR spectroscopy. The C/N ratio was significantly ($p<0.01$, rho=-0.88) correlated with CH_4 fluxes, but neither with production rates nor CO_2 fluxes. Inorganic (nitrate, sulfate, ferric iron) and organic (humic acids) electron acceptors together could explain differences in CH_4 production rates ($R^2=0.22$) whereas we did not find clear relationships between organic matter quality, methanogenic pathways (acetoclastic vs. hydrogenotrophic) and electron accepting capacity of the organic matter. Grain size distribution could sufficiently ($p<0.05$, rho=±0.65) explain differences in CH_4 fluxes. Surprisingly, sediment gas storage, potential production rates and water-atmosphere fluxes were decoupled from each other and did not show any correlations. Our results show that there exists a significant spatial variability of sediment gas production even within small lakes which can be explained by the origin and pre-processing, and therefore the degradability of the organic matter. We highlight that measuring production rates is not a suitable way to replace in-situ flux measurements as it neglects physical sediment properties and production and oxidation processes in the water column.

https://doi.org/10.5194/bg-2019-284
Preprint. Discussion started: 29 August 2019

1 Introduction

Inland waters play an important role in the global carbon cycle and contribute significantly to the natural emission of the greenhouse gases carbon dioxide (CO_2) and methane (CH_4) (Cole et al., 2007; Battin et al., 2009; Bastviken et al., 2011; Raymond et al., 2013; Regnier et al., 2013). Lakes and reservoirs are estimated to emit in total 0.32 – 0.39 Pg C of CO_2 and 0.58 Pg C (CO_2 -eq.) CH_4 year^{-1} (Cole et al., 2007; Bastviken et al., 2011; Raymond et al., 2013). Especially small lakes (< 0.1 km²) have been underestimated in the past in regard to their spatial expansion and therefore their contribution to global greenhouse gas emissions (Downing, 2010). Although small lakes account for approx. 1/3 of the total lake area and cover less than 1% of the global land surface, they contribute 35% of CO_2 and 72% of CH_4 emissions from lakes worldwide (Downing et al., 2006; Holgerson and Raymond, 2016). Even if the highest number of lakes can be found in boreal zones, the largest areas occur in lower latitudes around 50° (Verpoorter et al., 2014). Due to their shallowness, shorter water residence times and a smaller perimeter to volume ratio, metabolic processes and carbon (C) turnover in small lakes is much faster compared to larger lakes and they can therefore be expected to be more vulnerable to environmental and climatic change than the latter (Wetzel, 1992; Downing, 2010).

Recently, many studies have shown that both CO_2 and CH_4 fluxes are highly variable both on a spatial and temporal scale, but the majority of these measurements has been taken out on larger lakes and is concentrated in boreal regions (Schilder et al., 2013; Wik et al., 2013; Bastviken et al., 2015; Natchimuthu et al., 2016; Natchimuthu et al., 2017; Spafford and Risk, 2018). Beyond that, studies on gas production processes in the sediments, and studies linking sediment gas production to emissions both remain scarce. Nevertheless, anoxic sediments play a crucial role in-lake C cycling as they are the main producer of CO_2 and CH_4 which is subsequently released through the water column to the atmosphere. To understand the spatial patterns of CO_2 and CH_4 emissions, it is therefore crucial to understand CO_2 and CH_4 production processes in the sediment as well as their major controls.

The degradability of OM, and therefore the amount of produced CO_2 and CH_4, is mainly depending on its components, the microbial biomass and enzyme activities (Updegraff et al., 1995; McLatchey and Reddy, 1998; Fenchel et al., 2012). While C/N ratios can be used to determine the origin and the degradation state of OM, Fourier-transformed infrared (FTIR) spectroscopy can provide qualitative information about OM components and therefore its grade of decomposition (Meyers, 1994; Broder et al., 2012; Biester et al., 2014; Li et al., 2016). Artz et al. (2008) compiled a range of functional moieties that is used to characterize OM in peat soils but is also applicable to OM in general. While polysaccharides and proteins are preferentially degraded by microorganisms, cellulose or aromatic compounds (e.g. lignin) are due to their molecular structure more recalcitrant and therefore accumulate in the anoxic sediment (Fenchel et al., 2012; Tfaily et al., 2014). The prevalence of different OM compounds leads to specific FTIR spectra, as functional moieties have wavelength-specific absorption maxima (Niemeyer et al., 1992; Cocozza et al., 2003).

https://doi.org/10.5194/bg-2019-284
Preprint. Discussion started: 29 August 2019

In anoxic sediments, CO_2 and CH_4 are produced during breakdown of OM over a cascade of microbially induced processes. After the fermentation of complex organic polymers which mainly produces hydrogen (H_2) and OM of low molecular weight (e.g. acetate), the latter are being further oxidized to CO_2 together with a set of electron acceptors (nitrate, sulfate, ferric iron or humic substances) before CH_4 production initiates as the final step of terminal electron accepting processes after depletion of all other, thermodynamically more favorable electron acceptors. CH_4 in turn is mainly produced via two different pathways, the acetoclastic and the hydrogenotrophic pathway with either acetate (R1) or H_2 as substrate and CO_2 as electron acceptor (R2) (Conrad, 1999; Whiticar, 1999).

$CH_3COOH \rightarrow CO_2 + CH_4$ $\quad\quad \Delta\ G_r^0$ (25°C) = -50.99 kJ mol^{-1} $\quad\quad$ R1

$CO_2 + 4\ H_2 \rightarrow 2\ H_2O + CH_4$ $\quad\quad \Delta\ G_r^0$ (25°C) = -193.03 kJ mol^{-1} $\quad\quad$ R2

Several studies have shown that in anoxic wetland and marine sediments rich in labile organic compounds the acetoclastic pathway, which is energetically more favorable for microorganisms, dominates, whereas with increasing recalcitrance, the hydrogenotrophic pathway becomes more important as acetate as direct precursor of CH_4 gets depleted (Schoell, 1988; Hornibrook et al., 1997; Miyajima et al., 1997). Lojen et al. (1999) suggested that seasonal changes in the dominant methane pathway in a lake sediment are attributed to OM quality.

Whereas the potential of inorganic electron acceptors to suppress methanogenic activity is well studied (Yao et al., 1999; Fenchel et al., 2012), information on the role of humic substances as organic electron acceptors remain scarce. Klüpfel et al. (2014) revealed the potential of humic substances to be reduced and re-oxidized at oxic-anoxic interfaces in peatlands, sediments or soils underlying water table fluctuations and it has recently been shown that availability of EAC in OM controls CO_2 and CH_4 production in peat soils poor in inorganic EAs (Gao et al., 2019). As sediments from the lake under study here are also rich in OM, we wanted to verify if electron accepting (EAC) and donating capacities (EDC) of humic substances also play a role in explaining spatial variabilities of CO_2 and CH_4 production in lake sediments that are not subjected to water table fluctuations but might to a small extent in the upper parts of the sediments be influenced by oxygen from the water column due to the in our case prevalent perennial circulation (Lau et al., 2016).

The amount of CO_2 and CH_4 produced is therefore either depending on the availability and degradability of the OM itself, the presence of EAs and the concentration of H_2 and acetate as substrates for methanogenesis (Segers, 1998; Conrad, 1999; Megonigal et al., 2003; Blodau, 2011; Fenchel et al., 2012).

The spatial distribution of OM and sediment properties within lakes has been found to be highly variable in terms of their origin (terrestrial vs. aquatic), degradability, elemental geochemistry and grain size (Muri and Wakeham, 2006; Ostrovsky and Tęgowski, 2010; Tolu et al., 2017). It has also been shown that sediment grain size is an important factor for the evolution of CH4 bubbles in sediments (Ostrovsky

https://doi.org/10.5194/bg-2019-284
Preprint. Discussion started: 29 August 2019

and Tęgowski, 2010; Liu et al., 2018). Liu et al. (2016) for example revealed a decrease in CH4 ebullition with increased shares of sand in lake sediments. CH4 ebullition in turn is accountable for a large proportion (75%) of CH4 emissions from lakes (Bastviken et al., 2011).

So far, experimental incubations of lake sediments were only conducted with samples from one or few sites within one lake, rather comparing different lakes with each other than to study within-lake variations of CO_2 and CH_4 production and with a focus on temperature effects on production rates (Duc et al., 2010; Gudasz et al., 2010; Gudasz et al., 2015; Fuchs et al., 2016). Although a broad range of controls on CO_2 and CH_4 production has been widely investigated for anoxic peatland soils, studies on lake sediment are rare. To our knowledge, controls such as organic matter (OM) quality, the occurrence of alternative electron acceptors (EAs), thermodynamic processes and sediment grain size have not, or only individually, been systematically surveyed.

To close this knowledge gap, we determined the magnitude and spatial variability of sediment CO_2 and CH_4 production in a small and shallow temperate lake, and connected productions patterns to OM and sediment characteristics, thermodynamics, and water-atmosphere fluxes. To this end, we conducted slurry and intact sediment mesocosm incubations with sediment from crater lake Windsborn in Germany. This site was chosen as a model system having a high sediment OM content (~30%), a very small catchment area and no surficial in- or outflows in order to keep influences from the surrounding area as small as possible.

We hypothesize that (I) there exists a noticeable spatial variability of CO_2 and CH_4 production in the sediment, (II) the variability of production rates is reflected in the flux patterns, and that (III) production rates, methanogenic pathways and flux patterns can be explained by OM degradability, the occurrence of organic and inorganic EAs, and grain size distribution or a combination of these factors.

https://doi.org/10.5194/bg-2019-284
Preprint. Discussion started: 29 August 2019

Biogeosciences
Discussions

2 Materials and Methods

2.1 Study site

The studied Lake Windsborn is a polymictic, small and shallow crater lake in the Volcanic Eifel, Rhineland Palatinate, south-west Germany and is part of the "Mosenberg" volcano group (see Fig. 1) (LfU, 2013). The climate is temperate with mean annual temperature of 8.3°C and 931 mm precipitation (multi-annual mean 1981-2010; DWD, 2019). Lake Windsborn is the only genuine crater lake north of the Alpes. It emerged approx. 29,000 years ago after a volcanic eruption when the top of the volcano was blast away and the newly formed crater was subsequently filled with water (LfU, 2013). The present lake arose around 1850, after drainage of the lake and the partial removal of the peat from the lake bottom (Kappes and Sinsch, 2005). The lake is part of a conservation area that was established in 1927 (Kappes and Sinsch, 2005). From 1950 until the 1990s, the lake was used a fishing ground, and was therefore stocked up with fish and limed (LfU, 2013). The lake is nearly circular and surrounded by a 20 to 30 meter high rampart which consists of an alternation of red-brown ashes, slag and lapilli from the eruption. Therefore, it has a very small catchment of only about 8 ha compared to the lake surface of 1.41 ha without any surficial in- and outflows and is only fed by groundwater and precipitation (LfU, 2013; Meyer, 2013). The maximum lake depth varies between 1.3 and 1.7 meters (Kappes and Sinsch, 2005). The area is underlain by devonic quartzite (Kampf, 2005).

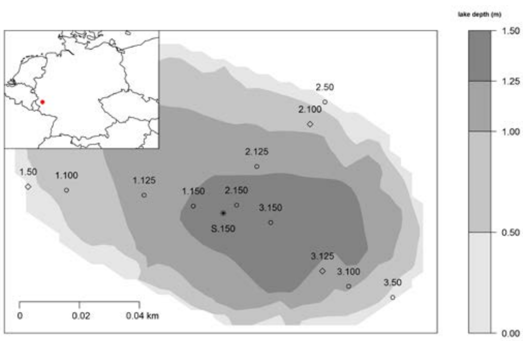

Figure 1: *Location of the study area and 13 sampling sites within Lake Windsborn. Rhombus: Sampling sites for incubations and sediment mesocosms, circles: sites for incubations only, asterisk: site for sediment mesocosm only (reference for 1.150, 2.150 and 3.150). Depths were interpolated by bivariate linear interpolation. Numbers 1, 2 and 3 refer to the number of transect from lake shore to center, numbers 50, 100, 125 and 150 indicate lake depth category (<50 cm, <100 cm, <125 cm, <150 cm).*

The lakes shoreline is vegetated with *Carex rostrata*, *Comarum palustre* and *Menynathes trifoliata*, all indicating poor nitrogen supply (Ellenberg et al., 2001). At the north-western riparian zone emerges a quaking bog of mainly *Sphagnum spec.* whose expansion will slowly lead to the silting up of the lake. Lake Windsborn was considered as humic-oligotrophic, but has transitioned to an eutrophic lake in the early 1990's now slowly recovering from human impacts and nutrient input (Kappes et al., 2000).

https://doi.org/10.5194/bg-2019-284
Preprint. Discussion started: 29 August 2019

Biogeosciences
Discussions
Open Access
EGU

During our measurement campaigns in 2017 and 2018, the lake exhibited partly meso- and eutrophic features as shown in Table 1.

Table 1: *Selected lake water characteristics measured in Lake Windsborn in 2017 and 2018. pH, conductivity and O2 concentration were determined in-situ, DOC and TN were determined by catalytic oxidation, chloride was determined by ion chromatography, and other elements by inductively coupled plasma optical emission spectroscopy (ICP-OES).*

parameter	**pH**	**cond.**	**O_2**	**Chlorophyll α**	**DOC**	**TN**	**Cl^-**
unit		µS cm^{-1}	mg L^{-1}	µg L^{-1}		mg L^{-1}	
n	*398*	*387*	*397*	*163*	*419*	*419*	*361*
average	6.8	19.35	9.67	27.67	13.74	0.96	2.86
± SD	0.84	1.72	0.91	18.66	2.30	1.89	3.44

parameter	**Ca**	**Fe**	**K**	**Mg**	**Na**	**P**	**S**
unit				mg L^{-1}			
n	*379*	*378*	*379*	*379*	*379*	*329*	*379*
average	1.17	0.11	0.77	0.72	4.01	0.06	0.41
± SD	0.27	0.06	0.42	0.13	5.01	0.06	0.13

2.2 Sediment incubations

2.2.1 Sampling and preparation of incubations

Samples for the incubation experiment were taken at three occasions in March, April and May 2018 from in total 12 locations within the lake from three transects covering multiple water depths (<50, <100, <125, and <150 cm) (see. Fig. 1). On each sampling date, four sampling sites were chosen randomly as it was not possible to set up the experiment with all samples at once. Measured air, water and sediment temperatures at the sampling dates were 7.7, 5.6 and 5.2 °C (March), 13.8, 15.1 and 10.1 °C (April) and 23.9, 23.6 and 13.8 °C (May). Sediment samples were taken in duplicates from a boat with a gravity corer (UWITEC, Mondsee, Austria) in 60 cm long PVC tubes and transported in an insulated box at ~5°C. Sediment cores were cut with a core cutter in the laboratory the next day in segments of 5 cm thickness (0-5 and 5-10 cm sediment depth). Duplicate samples were homogenized and then 20 g of each sediment was filled into 120 mL crimp vials added with 20 mL lake-water, and closed with a butyl-rubber stopper and aluminum crimp cap. Samples were flushed with nitrogen for 30 minutes in order to remove remaining oxygen from water and headspace, pre-incubated for one week to have them fully anoxic and then again flushed with nitrogen prior to the actual incubation. Incubations were set up in triplicates and stored at 25°C (corresponding to maximum measured in-situ sediment temperatures in summer 2018) in the dark. At each run, one set of parallel samples was incubated at 10°C in order to determine a Q_{10}-value for CO_2 and CH_4 production rates.

https://doi.org/10.5194/bg-2019-284
Preprint. Discussion started: 29 August 2019

The remaining sample material was freeze-dried (Alpha 1-4 LPplus, Christ, Osterode, Germany), ground with a ball mill (Mixer Mill MM 400, Retsch, Haan, Germany) and used for solid phase analyses as outlined below.

2.2.2 Sediment organic matter quality

Freeze-dried and ground sediment samples were analyzed for total carbon (C), nitrogen (N) and sulfur (S) concentrations and stable isotopes using isotope-ratio mass spectrometry (IRMS; Eurovector EA3000 coupled with Nu Instruments Nu Horizon, Hekatech, Wegberg, Germany) and for organic matter (OM) components using FTIR-Spectroscopy (Cary 670 FTIR Spectrometer, Agilent, Santa Clara, USA).

For IRMS, 5 mg of sample were weighed out into a tin cup together with 4 mg of Vanadium-Pentoxide (V2O5). The combustion and reduction furnace were set to 1000 and 650 °C, respectively, the resultant gaseous compounds were quantified by IRMS. Results are provided in % by mass for C, N and S contents and in ‰ vs. VPDB/AIR/VCDT for C, N and S isotopic signatures. For isotope analyses, appropriate certified reference materials were used: IAEA 600 ($\delta^{13}C$ = -27.771 ‰; $\delta^{15}N$ = 1.0 ‰) and S-1 ($\delta^{34}S$ = -0.30 ‰) for calibration, and BBOT (2.5-Bis-(5-tert.-butyl-2-benzo-oxazol-2-yl)thiophen; Hekatech, Wegberg, Germany), birch leaf, wheat flour and sorghum flour standards (IVA Analysetechnik e. K., Meerbusch, Germany) as working standards covering a range of -27.5 to -13.68 ‰ for ^{13}C, -0.6 to 2.12 ‰ for ^{15}N, and -9.3 to -1.42 ‰ for ^{34}S.

Functional groups of OM compounds were identified by FTIR spectroscopy. Therefore, 2 mg of freeze-dried sample were ground together with 200 mg KBr (potassium bromide) in a mortar, pressed to 13 mm pellets and analyzed. Each sample was scanned from 599 to 4000 cm^{-1} with a resolution of 2 cm^{-1} and baseline corrected. Distinct peaks at specific wavelengths were assigned to functional groups according to Artz et al. (2008) and normalized to the peak intensity at 1031 - 1035 cm^{-1} (indicative of polysaccharides) in order to obtain inter-comparable peak-ratios of functional moieties in all samples as FTIR spectra only provide information about relative abundance of certain functional moieties.

2.2.3 CO_2 and CH_4 production rates from incubations

Potential CO_2 and CH_4 productions rates were determined by measuring the increase in concentration of CO_2 and CH_4 in the incubation vials over time. Concentrations were obtained from analysis of the headspace at the beginning of the experiment (t0), and after 1, 3, 8, 11, 14 and 18 days (t1-t6). Samples were taken from the vial with a 10 mL PP syringe equipped with a 3-way-stopcock and 0.6 mm needle. Before each sampling, the pressure inside the vial was determined with a pressure sensor (GMH 3110, Greisinger, Regenstauf, Germany), and the syringe was three-times flushed with nitrogen, then 2 mL of nitrogen were left in the syringe before stabbing through the stopper, the nitrogen was added to the headspace, mixed, and subsequently 2 mL of sample were taken from the vial so that the volume inside the vial remained constant. The gas samples were analyzed for CO_2 and CH_4 concentrations with a gas chromatograph (8610 GC-TCD/FID, SRI Instruments, Torrance, USA) equipped with a Flame

https://doi.org/10.5194/bg-2019-284
Preprint. Discussion started: 29 August 2019

Biogeosciences Discussions
Open Access

Ionisation Detector (FID) and Methanizer to simultaneously measure CO_2 and CH_4. The gas chromatograph was calibrated with standard gas mixtures of known concentrations (CO_2: 385, 5,000 and 50,000 ppmV; CH_4: 5, 1,000 and 50,000 ppmV) before every sampling day.

First, measured concentrations in ppmV were pressure corrected and converted using the ideal gas law:

$$n = (p * V) / (R * T) \tag{1}$$

where n is the amount of substance in mol, p is the gas partial pressure in atm, V is the headspace volume in L, R is the ideal gas constant (0.082 L atm mol^{-1} K^{-1}) and T is the laboratory temperature in K.

Total CO_2 and CH_4 concentrations in gas and water phase in the incubation vials were calculated from headspace concentrations with Henry's Law:

$$c = K_h * p \tag{2}$$

where c is the concentration in the water phase in mol L^{-1}, K_h is the temperature-dependent Henry-constant (CO_2, 25°C = 0.0339 mol L^{-1} atm^{-1}, CH_4, 25°C = 0.00129 mol L^{-1} atm^{-1} (Sander, 2015)) and p is the gas partial pressure in atm.

Moreover, CO_2 concentrations were pH-corrected in order to obtain pH-independent values for total CO_2 concentrations using Henderson-Hasselbalch-equation and equilibrium constants according to Stumm and Morgan (1996):

$$n_{\Sigma CO2} = n_{water} * 10^{pH-6.4} + (n_{water} * 10^{pH-6.4}) * 10^{pH-10.25} \tag{3}$$

where $n_{\Sigma CO2}$ is the pH-corrected CO_2 amount in mol, and n_{water} is the calculated amount of CO_2 in the water phase in mol.

Finally, production rates were calculated as linear regression ($R^2 > 0.8$ for CO_2 and > 0.9 for CH_4) from concentration change over time.

To evaluate the effect of temperature on CO_2 and CH_4 production, we calculated Q_{10}-values, describing the relative increase of production rates with an increase in temperature of 10 Kelvin (Fenchel et al., 2012).

$$Q_{10} = (R2/R1)^{[10/(T2-T1)]} \tag{4}$$

where R2 is the production rate at T2 (25°C), and R1 is the production rate at T1 (10°C).

2.2.4 Thermodynamics and methanogenic pathways

In order to calculate the thermodynamic energy yield for hydrogenotrophic and acetoclastic methanogenesis we measured hydrogen (H_2) concentrations at the beginning (t0), after 8 days (t3) and at the end (t6) of the experiment and acetate (H_3COO^-) concentrations at the beginning and at the end of

https://doi.org/10.5194/bg-2019-284
Preprint. Discussion started: 29 August 2019

the incubation. The thermodynamic energy yield, expressed as Gibb's free energy was calculated using the Nernst equation as described in Beer and Blodau (2007):

$$\Delta G_r = \Delta G_r^0 + R * T \ln (\Pi_i(\text{products})^{vi} / \Pi_i(\text{educts})^{vi}) \quad (5)$$

By calculating the Gibb's free energy (ΔG_r), it is possible to evaluate whether these processes are feasible under given conditions. Therefore a theoretical threshold of -20 to -25 kJ mol^{-1} for has to be exceeded (Schink, 1997; Conrad, 1999; Blodau, 2011).

For H_2 concentration measurements, 2 mL of sample were taken from the incubation headspace with a syringe and needle and replaced with the same amount of N2. Samples were analyzed with a Reduction Gas Detector (RGD) Hydrogen and Carbon Monoxide Analyzer (ta3000R Gas Analyzer, Ametek, Pittsburgh, USA) that was calibrated with gas standards of 5, 25, and 50 ppmV H_2. Measured H_2 concentrations were corrected for pressure and converted into dissolved concentrations using Henry's Law ($K_h(H_2, 25°C) = 0.00078$ mol L^{-1} atm^{-1} (Sander, 2015)) analogous to CO_2 and CH_4.

Acetate concentrations were determined by ion chromatography IC with chemical suppression (883 Basic IC plus, Metrohm, Filderstadt, Germany; A-supp 5 column, Metrohm, Filderstadt, Germany). Aqueous samples were filtered with 0.45 µm Nylon + Glass Micro Fibre syringe filters (Simplepure, BGB Analytik, Rheinfelden, Germany) and kept frozen at -21°C until analysis.

2.2.5 Alternative Electron Acceptors

To quantify alternative Electron Acceptors (EAs) that could support anaerobic respiration and potentially suppress methanogenesis in anoxic incubations, we analyzed for nitrate (NO_3^-), sulfate (SO_4^{2-}), iron (III) (Fe^{3+}), and electron accepting and donating capacity of the organic matter (EAC/EDC_{OM}) at the beginning (t0) and the end (t6) of the incubation.

As the analysis of EAC_{OM} and EDC_{OM} is so far only possible on finely ground materials, providing potential capacities rather than true in-situ capacities, a second set of incubations for a sediment depth of 0-5 cm with samples from 10 sites (except 3.50 and 3.100) was set up with 0.4 g of the freeze-dried sediment material and 100 mL of Millipore water. Incubations were set up in six replicates, flushed with N2, pre-incubated and stored analogous to the first set of incubations. Samples were measured at the beginning and at the end of the experiment, whereas at every sampling occasion, three of the replicates had to be sacrificed (destructive sampling). To this end, samples were transferred into a glovebox (O_2 < 1 ppm, Innovative Technology, Amesbury, USA) prior to analysis to avoid alteration of the samples' redox state.

EAC_{OM} and EDC_{OM} were measured chronoamperometrically (CHI1000C, CH Instruments, Austin, USA) by mediated electrochemical reduction (MER) and oxidation (MEO) (Aeschbacher et al., 2010; Klüpfel et al., 2014). The cell consisted of a cylindrical glassy carbon working electrode, a Platinum wire counter electrode in a glass-ceramic frit, and an Ag/AgCl reference electrode. Cells were filled

https://doi.org/10.5194/bg-2019-284
Preprint. Discussion started: 29 August 2019

with 10 mL of 0.01 M/0.1 M MOPS/KCl-Buffer to stabilize the pH at 7 and continuously stirred during measurement. To facilitate electron transfer, organic mediators were added to the buffer; 180 µL DQ (diaquat-dibromide monohydrate, Sigma-Aldrich) for MER, and 180 µL ABTS (2,2'-azino-bis(3-ethylbenzthiazoline-sulfonic acid), Sigma-Aldrich) for MEO at a potential of E_h = -0.69 V and E_h = +0.41 V respectively (reported vs. the standard hydrogen electrode but experimentally measured vs. the Ag/AgCl reference electrode). To determine the electron transfer, 100 µL of suspended samples were added to the buffer solution (Lau et al., 2015), which resulted in an increase of the current recorded as a peak in the analysis software. After approx. 30 minutes, when the baseline was reached again, the next sample was added to the cells. Samples were measured in duplicates. The electron transfer was calculated with the Nernst-equation and normalized to the C content in the samples (Lau et al., 2015).

$$EAC_{OM} / EDC_{OM} = \text{peak area} / (V * F * C) \tag{6}$$

with EAC_{OM} /EDC_{OM} in µmol e^- gC^{-1}, peak area in µA sec, V = sample volume in µL, F = Faraday constant 96,485 A sec / mol e^-, and C = carbon content in mg L^{-1}.

EAC_{OM} and EDC_{OM} had to be corrected for Fe^{3+}, or iron (II) (Fe^{2+}) and sulfide (S^{2-}) concentrations respectively as with the applied potential also Fe^{3+} would be reduced and Fe^{2+} and S^{2-} oxidized (Lau et al., 2015; Agethen et al., 2018).

Fe^{2+}, Fe^{3+} and S^{2-} were determined colorimetrically (Gilboa-Garber, 1971; Tamura et al., 1974) with a spectrophotometer (Cary 100 UV-Vis, Agilent, Santa Clara, USA).

NO_3^- and SO_4^{2-} concentrations were determined with IC, as described above. Therefore, samples were filtered with a 0.45 µm syringe filter, filled in micro-centrifuge tubes, retrieved from the glovebox and frozen at -21°C until analysis.

Total electron accepting capacity (EAC_{tot}) was calculated as the sum of EAC_{OM} and EAC_{inorg} (EAC from nitrate, sulfate, iron (III)) considering the respective amounts of electrons transferred during main pathways of dissimilatory reduction (Konhauser, 2009):

$$EAC_{tot} = EAC_{OM} + NO_3^- * 5e^- + SO_4^{2-} * 8e^- + Fe^{3+} * 1e^- \tag{7}$$

In theory, EAC_{OM} and EDC_{OM} correlate with each other: if EAC_{OM} decreases, EDC_{OM} increases equivalently as quinones are reduced to hydroquinones. But in practice, values of EDC_{OM} are potentially biased as MEO does not only capture EDC_{OM}, but may also irreversibly oxidize phenolic moieties, which are sensitive to slightest changes in pH and potentials (Aeschbacher et al., 2011; Walpen et al., 2016; Walpen et al., 2018). The discussion will therefore focus on EAC_{OM} data.

2.3 Sediment mesocosms: CO_2 and CH_4 fluxes and sediment gas stock change

To obtain ex-situ CO_2 and CH_4 gas fluxes and estimate changes in sediment CO_2 and CH_4 stocks, intact sediment cores (PVC tubes, 60 cm length, 5.8 cm diameter) were taken in triplicates from four sites out of the twelve above in November 2017 (1.50, 2.100, 3.125, S.150; see Fig. 1). S.150 was chosen as one

https://doi.org/10.5194/bg-2019-284
Preprint. Discussion started: 29 August 2019

site representing the sites 1.150, 2.150 and 3.150 from the same lake depth category. Sediment cores were transported cooled and deployed in a climate chamber (CLF Plant Master, CLF Plant Climatics GmbH, Wertingen, Germany) at constant conditions (temperature 20°C, humidity 60 %). Cores were taken to ensure that each tube contained a sediment layer of on average 35 cm thickness, covered with a lake water column of 20 cm; in the lab we created a headspace of approx. 150 mL. The cores were equipped with eight sampling ports; one in the headspace, one in the water phase and six in the sediment. Of the latter, three were used to sample dissolved gases in the sediment, and three for sediment pore water extraction. The gas samplers consisted of a gas permeable silicon tubes of 5 cm length and 0.8 cm diameter equipped with a 3-way-stopcock, modified after Kammann et al. (2001). This technique allows for sampling of dissolved gases in the sediment by diffusive equilibration through the silicon membrane. For pore water sampling, a vacuum was applied with a syringe to suction samplers (Rhizon, Eijkelkamp Agrisearch, Giesbeek, Netherlands) of 5 cm length, 0.25 cm diameter, and about 0.1 µm pore size (Seeberg-Elverfeldt et al., 2005). Gas and pore water samplers were deployed in average depths of 5.0 ± 2.8, 15.3 ± 2.9, and 23.6 ± 2.1 cm below sediment surface.

All measurements were conducted after 50 days of incubation of the cores in the climate chamber when the system had reached a steady state as indicated by quasi-constant CO_2 and CH_4 concentrations in the sediment.

For the determination of CO_2 fluxes, the cores were closed gas-tight with a stopper and connected to a laser-based, portable greenhouse-gas analyzer (Los Gatos Research, San Jose, USA) which allowed to measure real-time increase of CO_2, CH_4 and H_2O concentrations in the headspace of the cores with a resolution of 1 Hz. As the headspace was too small for the instrument's flow rate, a gas bag with a volume of 150 mL was interposed between the headspace and the analyzer. The headspace was closed for 10 minutes, and the diffusive CO_2 flux was calculated by linear regression ($R^2 > 0.8$) of the increase in concentration over time and the ideal gas law, corrected for air pressure and temperature and related to the water surface area:

$$F = \Delta c/\Delta t * (p * V) / (A * R * T) \qquad (8)$$

where F is the CO_2 flux in µmol m^{-2} d^{-1}, $\Delta c/\Delta t$ is the slope of the linear regression in ppm d^{-1}, p is the air pressure in atm, V is the sum of headspace and gas bag volume in m^3, A is the water surface area in m^2, R is the ideal gas constant $8.2*10^{-5}$ m^3 atm mol^{-1} K^{-1}, and T is the temperature in K.

CH_4 fluxes were determined by closing the cores with the stopper for 24 hours, and taking a gas sample right after closing, and again after 24 hours with a syringe from the headspace. CH_4 fluxes were calculated according to Bastviken et al. (2004):

$$F(CH_4) = k * (C_w - C_{fc}) \qquad (9)$$

https://doi.org/10.5194/bg-2019-284
Preprint. Discussion started: 29 August 2019

where F is the CH_4 flux in mmol m^{-2} d^{-1}, k is the piston velocity in m d^{-1}, C_w is the measured CH_4 concentration in the water phase in mmol m^{-3} and C_{fc} is the CH_4 equilibrium concentration in the headspace at the given CH_4 water concentration.

The piston velocity k was determined as:

$$k = (-\ln((c_{sat} - c_{end})/(c_{sat} - c_{start}))/ \Delta t * V) / (A * K_h * R * T) \quad (10)$$

where c_{sat} is the saturation concentration in the chamber headspace at the measured CH_4 water concentration, c_{end} is the measured CH_4 concentration in the chamber headspace at the end of the flux measurement, c_{start} is the measured CH_4 concentration in the chamber headspace at the beginning of the flux measurement (all in µatm).

The flux was corrected for the non-linear increase of CH_4 concentration in the headspace over time due to saturation and divided into diffusive and ebullitive proportions based on the piston velocity ($k < 2$ = diffusion, $k > 2$ = ebullition).

CH_4 and CO_2 concentrations in the sediment were obtained from gas-permeable silicon tubes, determined by gas chromatography as described above (2.2.3) and calculated by Henry's Law using temperature corrected Henry's constants (see formula 4). Measured CO_2 concentrations were corrected for pH (formula 5).

The storage change of CO_2 and CH_4 in the sediment was calculated for each depth segment between two sampling ports as the difference between CH_4 concentrations obtained from silicon gas samples at the beginning and at the end of gas flux measurements:

$$\Delta CO_2/CH_4 = ((c(CO_2/CH_4)_{end} * V_{seg}) - (c(CO_2/CH_4)_{start} * V_{seg})) / \Delta t \quad (11)$$

where Δ CO_2/CH_4 is the storage change in mmol d^{-1}, $c(CO_2/CH_4)_{end/start}$ is the CO_2 / CH_4 sediment pore gas concentration at the end/beginning of the flux measurement in mmol m^{-3} and V_{seg} is the volume of the sediment core segment between two samplers in m³.

After completion of flux measurements, sediment mesocosms were eventually cut into 10 cm slices, freeze-dried and ground for solid phase analyses as described above.

2.4 Other chemical and physical parameters in water and sediment

Total phosphorus (P), sulphur (S), manganese (Mn) and iron (Fe) in the sediment were determined by wavelength dispersive X-ray fluorescence (WD-XRF; ZSX Primus II, Rigaku, Tokyo, Japan). To this end, 500 mg of freeze-dried and ground sample were pressed to pellets together with 50 mg of wax (Hoechst Wax C, Merck, Darmstadt, Germany) as pelleting agent. Calibration of the instrument was done using a set of 22 certified reference materials.

Dissolved organic carbon (DOC) and total nitrogen (TN) concentrations in watery samples and sediment pore water were determined by catalytic oxidation and subsequent NDIR detection with a total

https://doi.org/10.5194/bg-2019-284
Preprint. Discussion started: 29 August 2019

carbon/nitrogen analyzer (TOC-L/TNM-L, Shimadzu, Kyoto, Japan). Calibration was verified at each measurement day with potassium hydrogen phthalate (5 and 25 mg L^{-1}) and potassium nitrate (1 and 10 mg L^{-1}) standard solutions.

Grain size distribution was determined after Austrian standards (OENorm B 4412; OENorm L 1050; OENorm L 1061) by the Physio-geographic Lab of the Institute of Geography and Regional Research of the University of Vienna. To this end, the organic substance was removed from the samples with hydrogen peroxide (H_2O_2) prior to analyses and mineral fine soil was divided into clay (< 2 µm), silt (fine (2-6 µm), medium (6-20 µm), coarse (20-63 µm)) and sand (fine (63-200 µm), medium (200-630 µm), coarse (630-2000 µm)).

2.5 Statistics

All statistical analyses were conducted with R Studio, Version 3.5. 2 (R Core Team, 2018). Data was tested for normal distribution and homoscedasticity with Shapiro-Wilk and Levene- Test (Fox and Weisberg, 2011) respectively. For non-normally distributed data, significant differences between groups were identified using Kruskal-Wallis and Post-hoc Dunn- Test (Dinno, 2017) for more than two groups and Mann-Whitney-Test for comparing two groups. If the condition of homoscedasticity was not fulfilled, groups were compared with Mood's Median Test. Correlations and regressions between production rates and sediment parameters were calculated by Spearman's Rank Correlation and by linear regression models respectively. All data was tested on a 95% confidence interval and significance level of $\alpha = 0.05$.

https://doi.org/10.5194/bg-2019-284
Preprint. Discussion started: 29 August 2019

3 Results

3.1 Sediment incubations

3.1.1 Sediment Organic Matter Quality

The C content in the samples was between 2.15 and 33.16% with lowest values at site 3.50 and highest at site 1.50. C/N ratios ranged from 10.97 at site 1.150 to 19.06 at site 3.100. Neither C content nor C/N ratio showed significant changes with sediment nor lake depth, but C/N ratio was significantly higher in samples taken close to the shore (50) than in samples from the lake center (150) ($p < 0.01$).

Organic matter quality as identified by FTIR-analysis was predominated by strong absorption features of polysaccharides, lignin, humic acids, phenolic and aliphatic structures, aromatic compounds, and fats, waxes and lipids (see Fig. S1). Except for lignin, which was not identified at sites 2.50, 2.100, 2.125, 3.50, and 3.100, all components were found at all sites. Ranges of peak ratios for every component can be found in Tab. 2. Overall, lowest peak ratios were present at site 3.50 and highest at site 3.125, corresponding to highest and lowest CH_4 production rates. All peak ratios correlated with each other. They tended to increase with sediment depth and towards the lake center, respectively, but this change was not significant.

Table 2: *C, N, P, S, Mn, and Fe contents, C/N and FTIR peak ratios of identified OM compounds and their minimum and maximum values. n = 16-22.*

	Min	**Max**	**Average**
C (%)	2.15	33.16	26.45
N (%)	0.15	2.45	1.97
C/N ratio	10.97	19.06	13.81
$\delta^{13}C$ (‰)	-27.84	-27.3	-27.6
$\delta^{15}N$ (‰)	-6.27	1.33	-0.93
P (%)	0.3	0.51	0.37
S (%)	0.13	1.22	0.93
Mn (%)	0.037	0.12	0.049
Fe (%)	2.13	7.01	2.95
Lignin (1220-1234 cm^{-1})	0	0.437	0.235
Humic acids (1417-1419 cm^{-1})	0.039	0.491	0.328
Phenols & aliphatics (1456 cm^{-1})	0.018	0.480	0.324
Other Aromatics (1623-1646 cm^{-1})	0.210	0.825	0.629
Fats, waxes, lipids (2850-2856 cm^{-1})	0.178	0.492	0.349

https://doi.org/10.5194/bg-2019-284
Preprint. Discussion started: 29 August 2019

3.1.2 CO_2 and CH_4 production rates

Rates for potential CO_2 production in 0-5 cm depth ranged from 10.309 ± 0.003 µmol gC^{-1} d^{-1} at site 3.125 to 38.515 ± 2.48 µmol gC^{-1} d^{-1} at site 2.100. Potential CH_4 production lay between 7.3 ± 0.14 µmol gC^{-1} d^{-1} at site 3.125 and 33.53 ± 7.151 µmol gC^{-1} d^{-1} at site 3.50. Production rates in 5-10 cm depth were always lower compared to the upper sediment layer and were between 7.189 ± 0.072 and 14.714 ± 0.435 µmol gC^{-1} d^{-1} for CO_2 and between 5.361 ± 0.259 and 14.264 ± 0.341 gC^{-1} d^{-1} for CH_4. Both CO_2 and CH_4 production rates showed significant differences between sites (Kruskal-Wallis, $p < 0.001$) and were significantly (Dunn's, $p < 0.05$) higher at the shore (50+100) than in the center of the lake (125+150) (see Fig. 2 + Fig. S2).

CO_2 and CH_4 production rates decreased with time. CO_2 production was highest at the beginning, while CH_4 production had its peak after three to eight days of incubation (s. Fig. 3, Tab. 3). The CO_2/ CH_4 ratio constantly decreased during the incubation, with a maximum value of 62.13 ± 58.44 at the beginning of the incubation at site 1.125 and minimum values of 1.17 ± 0.004 at the end of the incubation at site 2.50 (s. also Tab. 3).

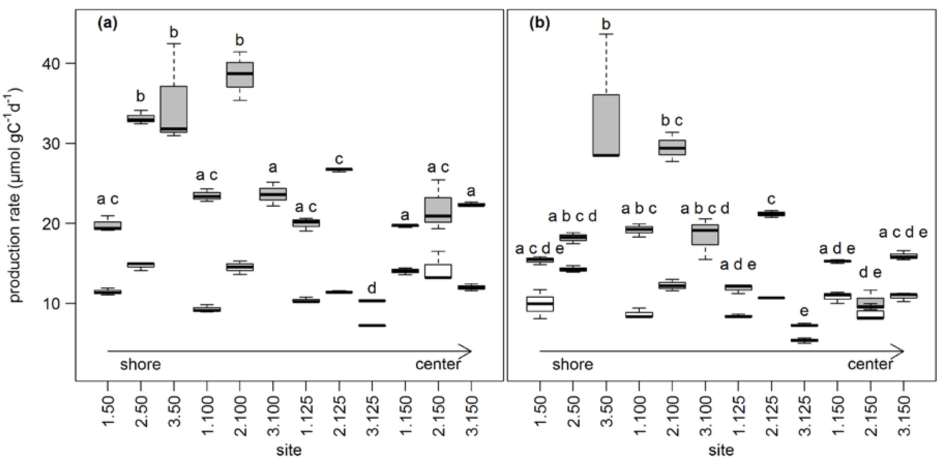

Figure 2: *CO_2 (a) and CH_4 (b) production rates in 0-5 (grey) and 5-10 (white) cm sediment depth. n = 3. Production rates are calculated from linear regression of concentration increase over time. Bold lines are the median, boxes show the 25 and 75 percentile, and whiskers indicate minima and maxima within 1.5 times the interquartile range. Different letters indicate significant differences between these sites.*

https://doi.org/10.5194/bg-2019-284
Preprint. Discussion started: 29 August 2019

Biogeosciences Discussions
Open Access
EGU

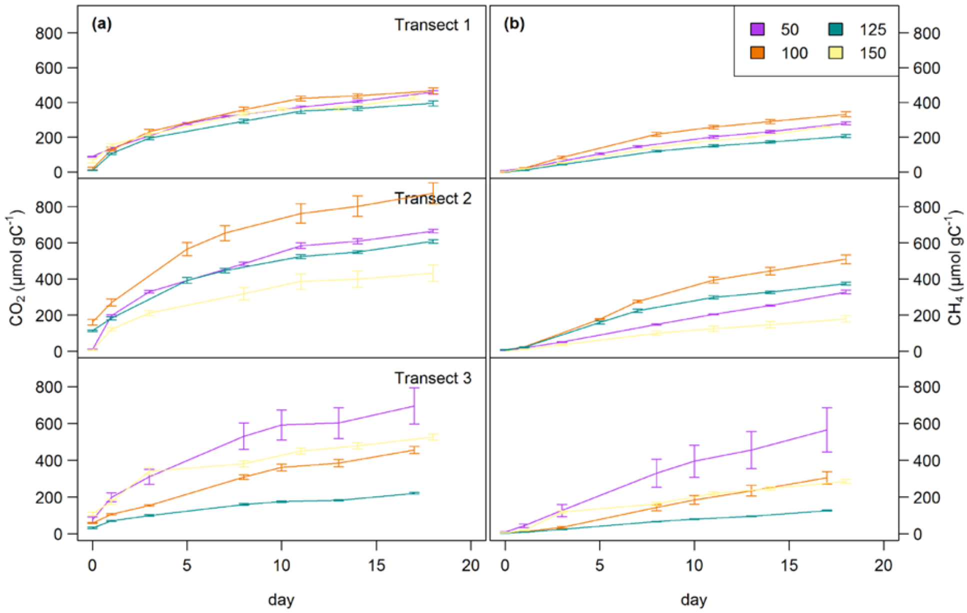

440

Figure 3: *CO_2 (a) and CH_4 (b) production over time at all sites in 0-5 cm sediment depth. Top: transect 1, middle: transect 2, bottom: transect 3. Line are average values of triplicate measurements ± SD.*

Table 3: *CO_2 and CH_4 production rates and CO_2/ CH_4 ratio over time. Rates are in µmol gC^{-1} d^{-1}, ratio is in µmol. Values in brackets are SDs.*

	sediment depth	**t0**	**t1**	**t2**	**t3**	**t4**	**t5**	**t6**
CO_2 production rate	0-5 cm		91.49 (40.29)	44.67 (16.77)	26.49 (9.69)	21.14 (7.59)	6.79 (3.59)	13.32 (5.00)
	5-10 cm		39.86 (14.18)	19.63 (5.95)	11.01 (2.69)	11.40 (3.06)	6.00 (2.20)	8.91 (2.74)
CH_4 production rate	0-5 cm		14.37 (7.44)	22.80 (11.26)	23.88 (11.47)	16.74 (7.86)	11.60 (4.69)	13.58 (5.78)
	5-10 cm		9.36 (2.67)	11.68 (2.85)	11.56 (3.13)	9.72 (2.34)	7.89 (2.10)	9.32 (2.72)
CO_2/CH_4 ratio	0-5 cm	14.55 (6.71)	8.70 (2.26)	3.84 (1.32)	2.33 (0.48)	2.11 (0.45)	1.89 (0.37)	1.73 (0.30)
	5-10 cm	16.19 (24.90)	5.61 (1.60)	2.92 (0.88)	1.93 (0.35)	1.74 (0.34)	1.57 (0.25)	1.44 (0.20)

445

Q_{10}-values were between 1.56 ± 0.13 and 2.19 ± 0.14 for CO_2 production rates and between 2.65 ± 0.48 and 11.37 ± 0.96 for CH_4.

Sampling dates did not have any impact on production rates as confirmed by Kruskal-Wallis-test (CH_4: p = 0.173, CO_2: p = 0.755)

https://doi.org/10.5194/bg-2019-284
Preprint. Discussion started: 29 August 2019

Neither CO_2 nor CH_4 production rates were correlated with C content or C/N ratio, but we found significant negative correlations ($p < 0.01$, rho < -0.6) between all peak ratios and CO_2 and CH_4 production rates as well as with Q10-values of CH_4 production ($p < 0.05$, rho = -0.82) (see Fig. 4).

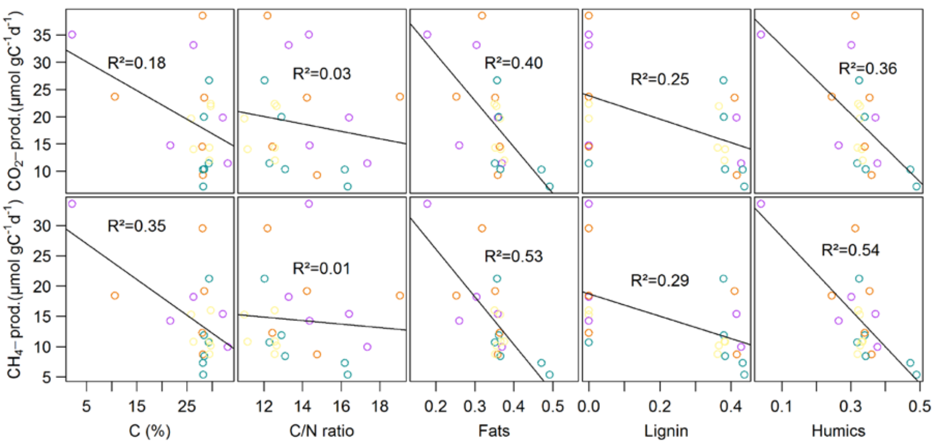

Figure 4: *Correlations between CO_2 and CH_4 production rates and OM quality parameters.*

3.1.3 Methanogenic pathways

Both H_2 and acetate concentrations increased during the incubation. H_2 concentrations were between 0 and 1587.42 ± 170.12 nmol L^{-1} and acetate concentrations ranged from 219.74 ± 104.25 to 1212.71 ± 11.35 µmol L^{-1} (see Fig. 5). Gibb's free energy for acetoclastic methanogenesis was between - 96.32 ± 0.84 and -66.37 ± 0.28 kJ mol^{-1} and for hydrogenotrophic methanogenesis between -62.41 ± 0.85 and -7.41 ± 0 kJ mol^{-1}. Energy yields decreased for the acetoclastic pathway and significantly (Mood's median, t0-t6: $p < 0.05$, t3-t6: $p < 0.001$) increased for the hydrogenotrophic pathway throughout the incubation (see Fig. 5). Energy yields did not differ between lake depths except for the acetoclastic pathway at the end of the incubation (t6, $p < 0.001$), when the energy yield was highest in samples from the center of the lake. Significant differences between all sites were found for the acetoclastic and hydrogenotrophic pathway at the beginning of the incubation (Kruskal-Wallis, $p < 0.01$) and at t6 for acetoclastic methanogenesis only (Kruskal-Wallis, $p < 0.01$). H_2 concentrations at the end of the experiment were significantly correlated with average CO_2 ($p < 0.001$, rho = +0.51) and CH_4 ($p < 0.001$, rho = +0.45) production rates. Further, Gibb's free energy of acetoclastic methanogenesis was positively correlated with C/N ratio ($p < 0.05$, rho = +0.45) at the end of the experiment (t6).

https://doi.org/10.5194/bg-2019-284
Preprint. Discussion started: 29 August 2019

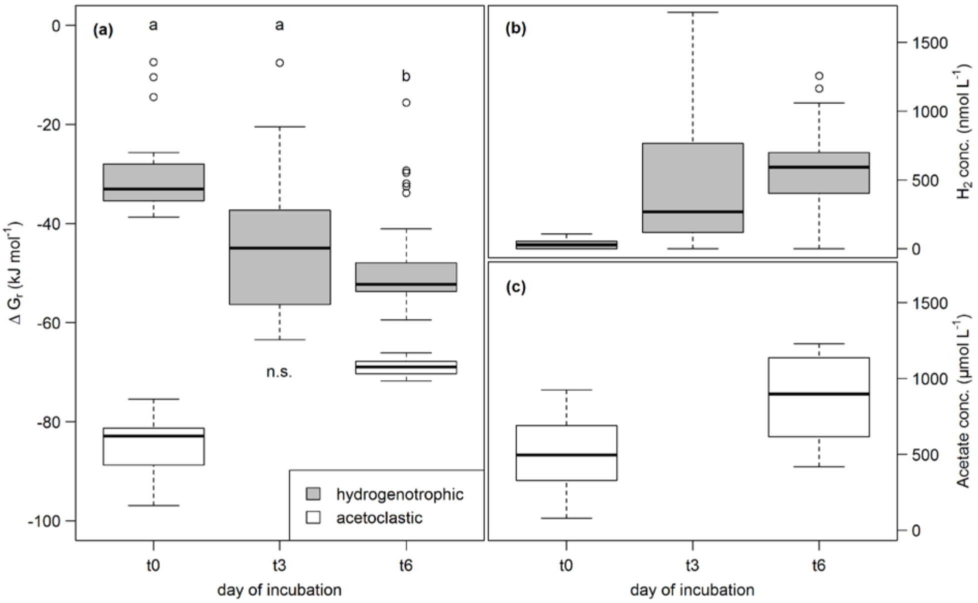

Figure 5: *(a) Change of Gibb's free energy of hydrogenotrophic (grey) and acetoclastic (white) methanogenesis and of H_2 (b) and acetate (c) concentrations over time. More negative ΔG_r values correspond to a higher energy yield. Different letters denote significant differences between sampling dates.*

3.1.4 Alternative Organic and Inorganic Electron Acceptors

EAC_{OM} lay between 218.69 ± 97.15 and 545.71 ± 60.33 µmol e^- gC^{-1} at t0 and decreased by an average of 44.85 µmol e^- gC^{-1} to 170.76 ± 32.70 to 460.79 ± 51.47 µmol e^- gC^{-1} at t6 with highest values found at site 3.125 corresponding to lowest measured CH_4 production rates at that site. EAC_{inorg} was, with values between 19.82 ± 10.52 and 218.01 ± 24.79 µmol e^- gC^{-1}, lower than EAC_{OM} and also decreased during the incubation by a mean of 42.40 µmol e^- gC^{-1}. EAC_{tot} ranged from 226.95 ± 83.87 µmol e^- gC^{-1} at site 3.150 to 614.58 ± 80.72 µmol e^- gC^{-1} at site 3.125 and significantly (t-test, $p < 0.001$) decreased by averagely 87.25 µmol e^- gC^{-1} from t0 to t6. EDC_{OM} was between 149.54 ± 26.72 and 462.69 ± 18.57 µmol e^- gC^{-1} at the beginning and between 152.94 ± 53.78 and 370.65 ± 196.22 µmol e^- gC^{-1} at the end of the incubation with a slight increase by on average 31.38 µmol e^- gC^{-1}. Lowest EDC_{OM} at both t0 and t6 was found at site 2.100, corresponding to highest CO_2 production rates there (see Fig. 6).

We further found significant differences for EAC_{OM} (ANOVA, $p < 0.001$) and EAC_{tot} (ANOVA, $p < 0.01$) between all sites with highest average values at site 3.125 and lowest at site 3.150 (see Fig. S3).

https://doi.org/10.5194/bg-2019-284
Preprint. Discussion started: 29 August 2019

Average CO_2 and CH_4 production rates were significantly ($p < 0.05$, rho = 0.7) negative correlated with initial EDC_{OM}, whereas we did not find any significant correlation with EAC, EEC nor EAC/EDC ratio, although low CH_4 production rates were associated with high EAC.

CO_2, CH_4 and acetate concentration were significantly ($p < 0.05$, < 0.05, < 0.001) negative correlated with EAC_{tot}. Gibb's free energy of hydrogenotrophic methanogenesis was significantly ($p < 0.05$) positive and acetate concentration significantly ($p < 0.01$) negative correlated to EAC_{OM}.

We did not find any significant correlations between EAC or EDC and OM quality parameters except for the FTIR peak ratio indicative of fats and lipids and EDC_{OM} ($p < 0.05$, rho = -0.76).

Of the inorganic EAs, only total sulfur content in the sediment was significantly negative correlated with CH_4 production rates ($p < 0.05$).

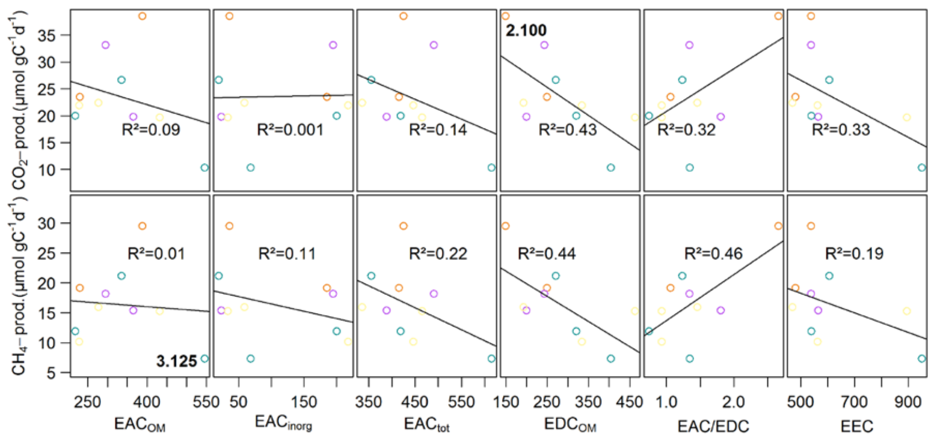

Figure 6: *Linear regression of CH_4 and CO_2 production rates with initial electron accepting and donating capacities. Points are mean values of triplicate measurements at each site.*

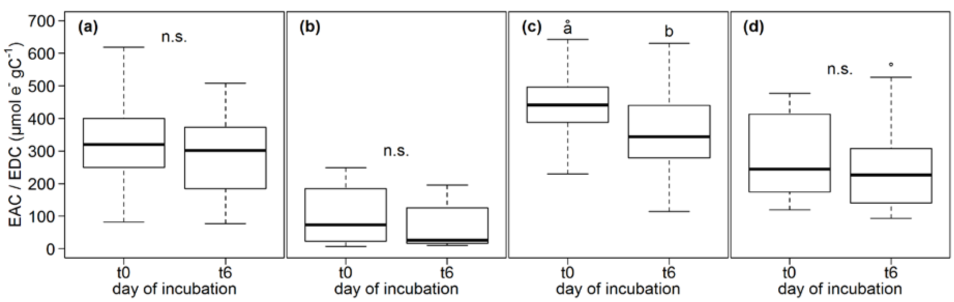

Figure 7: *EAC_{OM} (a), EAC_{inorg} (b), EAC_{tot} (c) and EDC_{OM} (d) at the beginning and the end of the incubation at all sites. n = 60-88. Different letters denote significant differences.*

https://doi.org/10.5194/bg-2019-284
Preprint. Discussion started: 29 August 2019

3.2 Sediment mesocosms: Fluxes, sediment storage change and grain size

CO_2 and CH_4 fluxes measured from sediment mesocosms ranged from 4.46 to 26.9 and 0 to 9.8 mmol m^{-2} d^{-1} respectively. CH_4 ebullition played a major role in cores from sites 2.100 and S.150 and accounted for up to 100% of the fluxes there. CO_2 fluxes at site 3.125 were significantly (t-test, $p < 0.05$) lower than at the other sites while total CH_4 fluxes at site 2.100 were significantly (Kruskal-Wallis, $p < 0.01$) higher compared to all other sites. Fluxes were within the same range like potential production rates in incubations but did only partly follow the pattern observed in incubations (see Fig. 8).

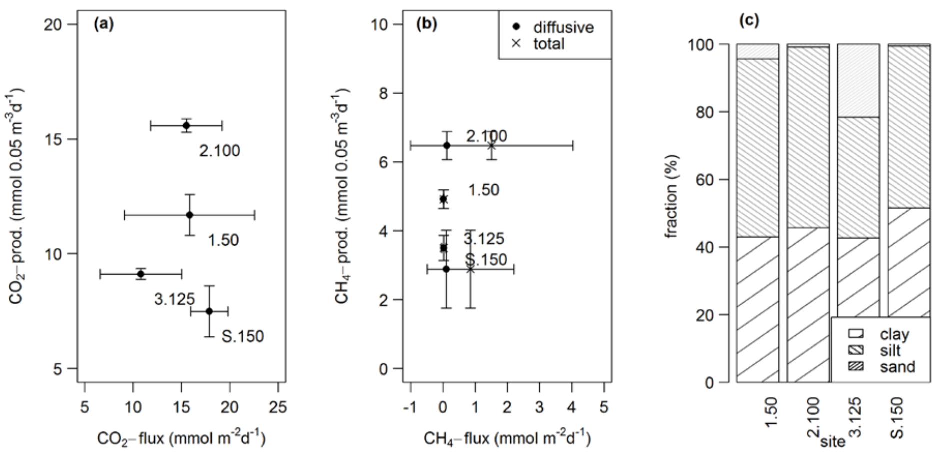

Figure 8: *Comparison of fluxes obtained from sediment mesocosms and potential production rates from the incubations (in 0-5 cm sediment depth) for CO_2 (a) and diffusive and total CH_4 (b). Points are averages (n(incubations) = 3-9, n(CO_2 fluxes) = 9-14, n(CH_4 fluxes) = 11-13), horizontal and vertical lines are standard deviations. We decided to display production rates from 0-5 cm sediment depth as this depth turned out to be most important for sediment gas production (see sections 3.1.2 & 4.1.2). (c) Relative grain size distribution in sediment mesocosms.*

https://doi.org/10.5194/bg-2019-284
Preprint. Discussion started: 29 August 2019

Table 4: *Spearman's rank correlation coefficients for CH_4 and CO_2 fluxes (means of each sediment mesocosm) and different sediment characteristics.*

	CH_4 flux		**CO_2 flux**	
	rho	p	rho	p
Clay	0.6477503	0.02275	0.6045669	0.03731
Silt	0.4966085	*n.s.*	0.3022835	*n.s.*
Sand	-0.6477503	0.02275	-0.6045669	0.03731
Fats, waxes, lipids	-0.8333333	0.01538	-0.3333333	*n.s.*
Phenols; humics	-0.8333333	0.01538	-0.3571429	*n.s.*
Aromates	-0.5952381	*n.s.*	-0.5238095	*n.s.*
Lignin	-0.7863867	0.02063	-0.3805097	*n.s.*
C/N	-0.8809524	0.007242	-0.3333333	*n.s.*
C (%)	-0.7142857	*n.s.*	-0.1904762	*n.s.*
CH_4 sediment stock change	-0.2219706	*n.s.*	0.04985994	*n.s.*
CO_2 sediment stock change	-0.04872526	*n.s.*	-0.06414566	*n.s.*

Concentrations of dissolved CH_4 and CO_2 ($\Sigma(CO_2, HCO_3^-, CO_3^{2-})$) in the sediment ranged from 3.97 to 129.45 mmol m^{-3} (CH_4) and from 322.92 to 3811.36 mmol m^{-3} (CO_2) respectively with lowest values found at site 3.125 and highest values at S.150. We did not see significant changes in CO_2 and CH_4 concentrations in the depth profile (see Fig. S4).

Observed changes of CH_4 and CO_2 concentration in the sediment of intact cores was overall very low and lay between 0.06 and 2.45 (CH_4) and 0.55 and 57.11 mmol d^{-1} (CO_2) in the upper 5 cm of the sediment. It was within the same order of magnitude as measured fluxes but did not correlate with the latter.

Grain sizes distribution differed between the four sites, with site 3.125 having the highest share of sand (21.6%) and lowest shares of silt and clay (35.68 and 42.73%) whereas the other sites were dominated by finer material and consisted of less than 5% of sandy components (see Fig. 8). CH_4 and CO_2 fluxes were significantly correlated with clay and sand content, but not with silt (see Tab. 5).

Similar to incubations, CH_4 fluxes were significantly negative correlated with some FTIR peak ratios indicative of recalcitrant OM compounds as well as with C/N ratio but not with C content. CO_2 fluxes did not show any significant correlation with OM quality parameters at all (see Tab. 5).

https://doi.org/10.5194/bg-2019-284
Preprint. Discussion started: 29 August 2019

4 Discussion

4.1 Sediment incubations

4.1.1 Spatial variability of OM quality

In our study, we found higher C/N ratios in samples close to the lake shore and narrower ratios in the lake center indicating a predominant input of allochthonous (terrestrial) material at the shore and mainly sedimentation of autochthonous (aquatic) OM in the lake center (Meyers, 1994).

Besides C/N ratios, FTIR peak ratios revealed information about the OM composition and quality in Lake Windsborn. We found FTIR peak ratios for refractory components (lignin, aromatics, humics, phenols, and lipids) increasing towards the lake center, indicating increasing predominance of more recalcitrant OM with higher distance from the lake shore. At first sight, this was unexpected as allochthonous material is known to be richer in recalcitrant compounds like lignin or aromates compared to autochthonous biomass and therefore being effectively buried in lake sediments (Sobek et al., 2009). On the other hand, the internally produced material in the lake center has to bypass a deeper water column before reaching the sediment, meanwhile undergoing degradation processes and leading to more decomposed OM reaching the sediment (Meyers, 1994; Torres et al., 2011). The less decomposed OM close to the shore might further originate from labile aquatic plant substrates growing at the shoreline (Wetzel, 1992; Cole et al., 2007).

Not only on a spatial scale, but also with sediment depth, C/N ratios decreased and FTIR peak ratios increased, corresponding with a decrease in CO_2 and CH_4 production rates. While sediment age typically increases, OM quality and thus reactivity usually decreases with sediment depth, as recalcitrant compounds are not being mineralized completely but instead buried and preserved in the sediment (Avnimelech et al., 1984; Burdige, 2007; Sobek et al., 2009).

4.1.2 Spatial variability and temperature dependency of CO_2 and CH_4 production rates

Our incubation experiment showed that both CO_2 and CH_4 production rates were highly variable within one lake of only small spatial extent. CH_4 production rates were within the range of formerly reported values from lakes in central Sweden, a reservoir in Brasil, and in sediments from Lakes Stechlin and Geneva in Germany and Switzerland (Duc et al., 2010; Fuchs et al., 2016; Grasset et al., 2018). CO_2 production rates were high compared to rates found in Lake Kinneret in Israel and in the Pantanal and Amazon regions in Brazil and exceeded reported values by a factor of 7 to 100 (Schwarz et al., 2008; Conrad et al., 2011). Compared to production rates after addition of fresh OM to lake sediment, our CO_2 and CH_4 production rates remained low (Grasset et al., 2018).

Both CO_2 and CH_4 production rates were higher in the topmost sediment layer compared to 5-10 cm sediment depth, suggesting that the first centimeters of the sediment play a major role for gas production as a consequence of temperature and microbial community distribution and changes in OM quality (as discussed below) (Falz et al., 1999; Sobek et al., 2009; Wilkinson et al., 2015).

https://doi.org/10.5194/bg-2019-284
Preprint. Discussion started: 29 August 2019

In all samples, production rates were higher at the beginning of the experiment than towards the end. While CO_2 production rates were highest right after the start and then constantly decreased until reaching a plateau around day 8, CH_4 production rates peaked after 3 to 8 days and then slowly decreased afterwards approaching a 1:1 CO_2:CH_4 production ratio. This typically observed 3-phase pattern (Yao et al., 1999) might e.g. be due to thermodynamic constraints, such as end product accumulation in the sample vials and subsequent inhibition of methanogenesis (Beer and Blodau, 2007; Blodau et al., 2011; Bonaiuti et al., 2017). The observed delay in notable CH_4 production can be explained by the prevalent alternative EAs (NO_3^-, Fe^{3+}, SO_4^{2-}, humic substances) suppressing methanogenic activity (Lovley et al., 1996; Yao et al., 1999; Fenchel et al., 2012).

Similar to den Heyer and Kalff (1998), we found higher production rates in samples close to the lake shore in contrast to lower production rates in the center, suggesting that either the input rate of OM to the sediment is higher and therefore fueling higher degradation rates or/and that the organic material at these sites is more labile and therefore more easily degradable for microorganisms. More details on that hypothesis will be given in the following.

The high measured variability in production rates showed that it is necessary to sample lake sediments from different locations in one lake, in order to understand potentials of CO_2 and CH_4 production representative of the whole lake and that upscaling production rates based on single point measurements may be highly biased. Considering only sediment production rates, it seems that the in other studies observed spatial variability of CO_2 and CH_4 emissions from lakes (Schilder et al., 2013; Bastviken et al., 2015; Natchimuthu et al., 2016; Natchimuthu et al., 2017; Spafford and Risk, 2018) might to a large extent be controlled by sediment gas production. But still, as sediment production and emission patterns have so far only been considered separately, important relations might have been neglected. In section 4.2, we therefore further discuss the relationships between CO_2 and CH_4 production and actual emissions and relate them to sediment properties.

Many studies revealed that higher temperatures lead to enhanced mineralization of OM due to higher microbial activity and thus increased production of CH_4 and CO_2 in sediments (den Heyer and Kalff, 1998; Sobek et al., 2009; Gudasz et al., 2015). Accordingly, we found that production rates of CO_2 were 2-times and of CH_4 2 to 11-times higher with a temperature increase of 10°C. Q_{10} values for CO_2 were within the range of earlier reported values by Liikanen et al. (2002) and Berström et al. (2010) whereas Q_{10} values for CH_4 production were slightly higher than values found by Duc et al. (2010). The high observed range of Q_{10}-values, especially for CH_4, implies that responses of temperature increase might not be homogeneously distributed within one single lake. The observed negative correlation between Q_{10}-values and OM quality indicators suggests that sites with more labile OM are more vulnerable to increasing temperatures in terms of CH_4 production and that at sites with more recalcitrant OM, the latter may limit the degradation processes. Aben et al. (2017) and Kiuru et al. (2018) showed that increasing temperatures caused higher CO_2 and CH_4 emissions from lakes. Assuming that gas

https://doi.org/10.5194/bg-2019-284
Preprint. Discussion started: 29 August 2019

production in the sediment and efflux to the atmosphere are coupled, global warming may thus drastically enhance emissions from small lakes like Lake Windsborn, especially regarding the fact that these sediments warm much faster (max. bottom-water temperature in summer 2018: 26.65°C, surface water temperature at the same time: 27.14 °C) compared to deeper lakes which have a deeper water column and stable thermal summer stratification as buffer (Jankowski et al., 2006).

4.1.3 Influence of OM quality on CO_2 and CH_4 production rates

The amount and the quality of OM usually determines the degradability and therefore the production of end-products of anaerobic mineralization processes, CO_2 and CH_4.

Against our expectations and previous findings e.g. by Conrad et al. (2011) and Romeijn et al. (2019), C content was not correlated with CO_2 nor CH_4 production rates. As the production potential is obviously not depending on the amount of C, we suggest that instead the OM quality might be the determining factor for CO_2 and CH_4 production.

Typically, OM of autochthonous origin fuels higher degradation rates than allochthonous OM (West et al., 2012; Grasset et al., 2018) as the latter is rich in compounds like lignin, cellulose and humic acids, being recalcitrant to decomposition and therefore being effectively buried in lake sediments (Sobek et al., 2009). We however measured higher CO_2 and CH_4 production rates at sites close to the shore receiving higher inputs of allochthonous material compared to the center of the lake receiving mainly autochthonous OM as indicated by the C/N ratio. As a wider C/N ratio does not only indicate OM of terrestrial origin, but also implies that the OM is still less decomposed and therefore has a higher decomposition potential whereas a narrower C/N ratio is not only typical of aquatic OM but also indicates a higher degradation state, higher production rates at sites closer to the shore seem to be reasonable (Malmer and Holm, 1984; Meyers, 1994; Kuhry and Vitt, 1996; Gudasz et al., 2015; Grasset et al., 2018). Anyway, the correlation between production rates and C/N ratio was not significant, implying that the C/N ratio might, due to before explained contradictions, not be a suitable proxy for the mineralization potential in our case. Instead, all FTIR peak ratios were significantly negative correlated with CO_2 and CH_4 production rates, supporting the hypothesis that OM mineralization is highly dependent on the quality of the OM.

To summarize, the quality of OM is not necessarily depending on its origin and that OM of terrestrial origin is not necessarily more recalcitrant to degradation by aquatic microorganisms. Sites closer to the shore probably receive higher rates of terrestrial OM matter being less decomposed, whereas autochthonous production in the lake center is overall low, due to the low nutrient status of the lake, and already undergoing degradation processes during sedimentation. This leads to more recalcitrant OM in the sediment. Earlier studies which found that allochthonous material is less decomposable compared to autochthonous matter were conducted in larger lakes, where the influence of the watershed is overall lower due to a lower perimeter to volume ratio. We hypothesize that in small and nutrient-poor lakes

https://doi.org/10.5194/bg-2019-284
Preprint. Discussion started: 29 August 2019

the pattern might be reversed as the system adapts to overall low productivity and simultaneous high input of terrestrially produced OM.

4.1.4 Methanogenic pathways

To make methanogenesis a profitable reaction for microorganisms, theoretical thresholds of -10.6 kJ mol^{-1} for the hydrogenotrophic and -12.8 kJ mol^{-1} for the acetoclastic pathway have to be exceeded (Hoehler et al., 2001). Except for a few samples at the beginning of the incubation, the theoretical thresholds were always exceeded, suggesting that both pathways contributed to CH_4 production. During the incubation, Gibb's free energy increased for the hydrogenotrophic pathway, implying an increasing contribution of that pathway to total CH_4 production, whereas it was opposite for the acetoclastic pathway. This suggests that labile organic polymers as precursors of acetate got depleted during the incubation so that H_2 gained of importance as substrate for methanogenesis. But when considering H_2 and acetate concentrations, the picture gets more complicated. An overall increase of H_2 concentrations was observed during incubation, but average H_2 concentrations at t3 had a high standard deviation (see Fig. 5) because some samples showed a peak in H_2 concentrations at t3 instead of a constant increase. These patterns could hint at an imbalance of the system, where fermenting, syntrophic and methanogenic bacteria were not yet equilibrated (Fey and Conrad, 2003). It is also remarkable, that the energy yield for acetoclastic methanogenesis decreased although acetate concentrations increased. We propose two different explanations for this finding: First, acetate is also used to reduce other EAs, which were present in higher concentrations at the beginning of the incubation, and therefore might have kept acetate concentrations low. Second, higher acetate concentrations do not necessarily mean more favorable thermodynamic conditions due to end product accumulation. During degradation of carbohydrates, H_2 and acetate are being produced in a 2:1 ratio. We found acetate concentration exceeding H_2 concentrations by a factor of 10^3, suggesting that homoacetogenesis contributed significantly to acetate production in our incubations (Conrad, 1999).

Against our expectations, Gibb's free energy of acetoclastic methanogenesis was significantly lowest in the center of the lake at t6 and was additionally positively correlated with C/N ratio. Considering that we found the lowest OM quality in the lake center and that low C/N ratio indicate OM of high recalcitrance whereas the acetoclastic pathway is attributed to predominate with high quality substrates, we would have expected a reverse pattern. Also, we found significant differences of energy yields between the sites, but could not relate them to OM quality. This implies that acetate as intermediate in the anaerobic OM mineralization cascade is not the rate determining step, but rather is fermentation and that OM quality only explains a part of the variance in CO_2 and CH_4 production patterns.

It further has to be mentioned, that correlations with CO_2 and CH_4 production rates were only observed for H_2 concentrations at the end of the incubation, but not with acetate. This finding emphasizes the hypothesis that the system was not in balance from the beginning of the incubation, and that fermentation seems to be the rate determining step for OM mineralization.

https://doi.org/10.5194/bg-2019-284
Preprint. Discussion started: 29 August 2019

4.1.5 Alternative electron acceptors

Average EAC_{OM} measured in our experiment (302.8 ± 124.6 µmol e^- gC^{-1}) was slightly lower but in the same order of magnitude compared to values found by Lau et al. (2015) and Gao et al. (2019) in peat soils and other lake sediments respectively. Given that C contents in the study by Gao et al. (2019) were much higher than in our study (46.2 – 49.4 %, Agethen and Knorr (2018)) and that Lau et al. (2015) fully oxidized their samples (C content 11.0 – 27.4 %), our measured capacities seem reasonable.

We found both organic and inorganic EAs decreasing during the experiment, indicating that EAs are being depleted with time as they are being reduced by microorganisms.

Sites with higher EAC_{tot} had lower CH_4 production rates and vice versa as increased concentration of oxidized humic substances would suppress methanogenic activity, supporting the findings of Agethen et al. (2018) and Gao et al. (2019). Although the relationship between EAC and CH_4 production was – probably due to the low number of samples - not significant, a clear trend was observable. Additionally, relationships were stronger with EAC_{tot} that with EAC_{inorg} or EAC_{org} only, suggesting that humic substances play a crucial, but variable role as terminal electron acceptors and should not be neglected when estimating the contribution of EAs to methanogenic activity in lake sediments rich in OM (~30%) (Lau et al., 2016). The spatial variability of measured EAC and C content in the samples shows that substrate composition is critical when evaluating the contribution of different EAs and CH_4 production patterns.

4.2 Comparison of production rates, fluxes, and sediment parameters

Comparing the order of magnitude of potential production rates from incubations and fluxes from intact sediment cores, results were in good accordance with each other. While CO_2 production rates were overall something below measured fluxes, CH_4 production rates were higher than CH_4 fluxes. The differences in CO_2 production rates and fluxes can be explained by the influence of the water column: CO_2 is not only produced in the sediment, but also in the water column, e.g. by the degradation of OM or zooplankton respiration (Kling et al., 1992) and can therefore contribute to water-atmosphere fluxes. The differences concerning CH_4 could be explained by several approaches. First, preparing incubations leads to the homogenization of the sediment and higher surface area, and therefore even distribution of substrates and microorganisms which is then better available for the latter (Hoehler et al., 2001). Secondly, sediment fluxes from intact sediment cores may be low compared to homogenized incubations as we did not observe significant increases in the depth profile of sediment cores and suggest that strong changes in sediment gas concentrations which are driving fluxes are likely to occur only in the upper mm to cm. Additionally, the preparation of incubations reduces thermodynamic constraints which usually exist in intact profiles due to end product accumulation (Blodau et al., 2011; Bonaiuti et al., 2017). Thirdly, not all CH_4 produced in and emitted by the sediment will reach the water-atmosphere interface because of consumption processes in the oxygenated water column that has to be passed.

https://doi.org/10.5194/bg-2019-284
Preprint. Discussion started: 29 August 2019

Through CH_4 oxidation in the water column, amounts of CH_4 emitted from lakes to the atmosphere can be substantially reduced by 51 to 100 % (Bastviken et al., 2002; Bastviken et al., 2008).

Interestingly, spatial patterns of CO_2 and CH_4 emissions could not be well reproduced from sediment incubations. Although highest CO_2 emissions were observed at site S.150, we found lowest CO_2 production rates there. Additionally, we did not see any correlations between sediment OM quality and CO_2 fluxes, suggesting that CO_2 production processes in the sediment overlying water column play a much more important role than in the sediment itself. Moreover CH_4 production rates at sites 1.50 and 3.125 differed significantly from each other while this was not the case when comparing fluxes. We assume that the different patterns of CH_4 fluxes and production can be explained by grain size distribution and thus physical sediment properties. Sediment grain size determines sediment pore size which is essential for the evolution of methane bubbles in the sediment (Boudreau et al., 2005). Ebullition is the major component of CH_4 fluxes in shallow waters as it can efficiently bypass oxidation in the water column (Bastviken et al., 2004; Wik et al., 2013; Natchimuthu et al., 2016). We found ebullition supporting significantly to total CH_4 fluxes in two of our four sediment mesocosms, whereas sites with higher shares of sand exhibited less ebullitive fluxes confirming the findings of Liu et al. (2016) and (2018). We further found OM quality being partly significantly correlated to CH_4 fluxes, but to a lesser extent than to CH_4 production. These findings suggest that grain size distribution is besides OM quality a main driver of spatial CH_4 flux patterns in mesocosms. On the other hand, when preparing incubations, the physical sediment structure is destroyed, so that OM quality becomes the major controlling factor for gas production. Although we also found OM quality being significantly correlated to mesocosm fluxes, we suppose that the combination of physical characteristics and sediment OM quality can sufficiently explain CH_4 emission patterns from lakes.

The missing link between sediment gas storage and both diffusive and ebullitive emissions could be explained by our sampling procedure. While fluxes were partly dominated by bubbles, these bubbles cannot be captured in the sediment by silicon samplers. Silicon samplers rely on the slow diffusion of gas between the pore gas and the sampler. Bubbles however may form on shorter time-scales and could quickly being released to the water-column. Thus, concentrations in the bulk sediment stay similar while the released bubbles cause high fluxes. Moreover, the resolution of our gas samplers was probably not high enough, not covering the uppermost centimeters of the sediment which we assume to be crucial for diffusive fluxes.

5 Conclusion

Our experiment showed that there exists a significant spatial variability of CO_2 and CH_4 production in the sediment of a small and shallow lake and that it is therefore not possible to upscale sediment production rates from single point measurements. We further proved that especially CH_4 production is strongly depending on temperature, and that the extent of temperature dependence might differ within one lake, especially between littoral and central parts due to different OM quality. Small lakes seem to

https://doi.org/10.5194/bg-2019-284
Preprint. Discussion started: 29 August 2019

be very vulnerable to temperature increases in terms of accelerated C cycling which implies they might become larger sources of CO_2 and CH_4 emissions under climate change scenarios. Still, they might not react homogeneously, but we could unroll that sediments in shallower parts might react more sensitively due to lower water columns and input of reactive allochthonous OM, which is particularly important for oligotrophic lakes without significant contribution of autochthonous primary production. The strong negative correlations we found between recalcitrant OM compounds and CO_2 and CH_4 production rates proved evidence that OM quality plays a major role in controlling the mineralization of anoxic lake sediment and can be used to explain and predict within-lake patterns of production rates. Both hydrogenotrophic and acetoclastic methanogenesis were feasible during incubations, but we could neither clearly refer observed patterns to OM quality nor electron exchange capacities, and therefore suggest that both H_2 and acetate were not limited as substrates but that fermentation was the rate-determining step of OM mineralization. More than organic or inorganic EAs alone, EAC_{tot} could explain observed variabilities in CH_4 production, implying that also organic EAs play a major role in constantly anoxic lake sediments with high C contents.

However, measured production rates were only partly reflected in CO_2 and CH_4 flux patterns obtained from whole core incubations. We suggest that this is due to the destruction of physical sediment parameters in the incubations (e.g. pore size) which are crucial for the evolution of CH_4 bubbles in the sediment and due to the lack of thermodynamic and gas transport constraints that exist in intact anoxic sediment profiles. Further, measuring production rates neglects the importance of the water column as a sink of sediment generated CH_4 through oxidation and source of CO_2 through degradation and respiration processes which might then cause discrepancies between observed production and flux rates.

So far, direct flux measurements of CO_2 and CH_4 between water and the atmosphere seem to be the most accurate way for determining the magnitude and variability of emissions from lakes, but still our study contributes substantially to the understanding of controls on CO_2 and CH_4 production processes in lake sediments.

https://doi.org/10.5194/bg-2019-284
Preprint. Discussion started: 29 August 2019

6 Data availability

The underlying research data of this study can be found in the Supplement.

7 Author contribution

LP, MS, SS, NP and KHK designed the study. NP and SS carried out the experiments and sample analyses with the help of LP and MS. LP performed data analyses and wrote the manuscript with the help of NP, SS, KHK and GB.

8 Competing interests

The authors declare that they have no conflict of interest.

9 Acknowledgements

We thank the technicians of the laboratory of the institute of landscape ecology Ulrike Berning-Mader, Madeleine Supper, Viktoria Ratachin and Melanie Tappe for sample measurements. We further thank Rebecca Pabst, Christina Hackmann, Fabian Lange, Isabelle Rieke, Friederike Ding, Victoria Tietz and Anja Radermacher for their assistance during laboratory work and Stephan Glatzel for grain size analyses. This project was funded by the German Research Foundation DFG (BL 563/25-1). We acknowledge support from the Open Access Publication Fund of the University of Muenster.

https://doi.org/10.5194/bg-2019-284
Preprint. Discussion started: 29 August 2019

10 References

Aben, R. C. H., Barros, N., van Donk, E., Frenken, T., Hilt, S., Kazanjian, G., Lamers, L. P. M., Peeters, E. T. H. M., Roelofs, J. G. M., Senerpont Domis, L. N. de, Stephan, S., Velthuis, M., van de Waal, D. B., Wik, M., Thornton, B. F., Wilkinson, J., DelSontro, T., and Kosten, S.: Cross continental increase in methane ebullition under climate change, Nature communications, 8, 1682, https://doi.org/10.1038/s41467-017-01535-y, 2017.

Aeschbacher, M., Vergari, D., Schwarzenbach, R. P., and Sander, M.: Electrochemical analysis of proton and electron transfer equilibria of the reducible moieties in humic acids, Environ. Sci. Technol., 45, 8385–8394, https://doi.org/10.1021/es201981g, 2011.

Aeschbacher, M., Sander, M., and Schwarzenbach, R. P.: Novel electrochemical approach to assess the redox properties of humic substances, Environmental science & technology, 44, 87–93, https://doi.org/10.1021/es902627p, 2010.

Agethen, S. and Knorr, K.-H.: Juncus effusus mono-stands in restored cutover peat bogs – Analysis of litter quality, controls of anaerobic decomposition, and the risk of secondary carbon loss, Soil Biology and Biochemistry, 117, 139–152, https://doi.org/10.1016/j.soilbio.2017.11.020, 2018.

Agethen, S., Sander, M., Waldemer, C., and Knorr, K.-H.: Plant rhizosphere oxidation reduces methane production and emission in rewetted peatlands, Soil Biology and Biochemistry, 125, 125–135, https://doi.org/10.1016/j.soilbio.2018.07.006, 2018.

Artz, R. R.E., Chapman, S. J., Jean Robertson, A. H., Potts, J. M., Laggoun-Défarge, F., Gogo, S., Comont, L., Disnar, J.-R., and Francez, A.-J.: FTIR spectroscopy can be used as a screening tool for organic matter quality in regenerating cutover peatlands, Soil Biology and Biochemistry, 40, 515–527, https://doi.org/10.1016/j.soilbio.2007.09.019, 2008.

Avnimelech, Y., McHenry, J. R., and Ross, J. D.: Decomposition of organic matter in lake sediments, Environmental science & technology, 18, 5–11, https://doi.org/10.1021/es00119a004, 1984.

Bastviken, D., Sundgren, I., Natchimuthu, S., Reyier, H., and Gålfalk, M.: Technical Note: Cost-efficient approaches to measure carbon dioxide (CO₂) fluxes and concentrations in terrestrial and aquatic environments using mini loggers, Biogeosciences, 12, 3849–3859, https://doi.org/10.5194/bg-12-3849-2015, 2015.

Bastviken, D., Tranvik, L. J., Downing, J. A., Crill, P. M., and Enrich-Prast, A.: Freshwater methane emissions offset the continental carbon sink, Science (New York, N.Y.), 331, 50, https://doi.org/10.1126/science.1196808, 2011.

Bastviken, D., Cole, J. J., Pace, M. L., and van de Bogert, M. C.: Fates of methane from different lake habitats: Connecting whole-lake budgets and CH 4 emissions, J. Geophys. Res. Biogeosci., 113, n/a-n/a, https://doi.org/10.1029/2007JG000608, 2008.

Bastviken, D., Cole, J., Pace, M., and Tranvik, L.: Methane emissions from lakes: Dependence of lake characteristics, two regional assessments, and a global estimate, Global Biogeochem. Cycles, 18, n/a-n/a, https://doi.org/10.1029/2004GB002238, 2004.

Bastviken, D., Ejlertsson, J., and Tranvik, L.: Measurement of Methane Oxidation in Lakes: A Comparison of Methods, Environ. Sci. Technol., 36, 3354–3361, https://doi.org/10.1021/es010311p, 2002.

Battin, T. J., Luyssaert, S., Kaplan, L. A., Aufdenkampe, A. K., Richter, A., and Tranvik, L. J.: The boundless carbon cycle, Nature Geosci, 2, 598–600, https://doi.org/10.1038/ngeo618, 2009.

Beer, J. and Blodau, C.: Transport and thermodynamics constrain belowground carbon turnover in a northern peatland, Geochimica et Cosmochimica Acta, 71, 2989–3002, https://doi.org/10.1016/j.gca.2007.03.010, 2007.

Berström, I., Kortelainen, P., Sarvala, J., and Salonen, K.: Effects of temperature and sediment properties on benthic CO 2 production in an oligotrophic boreal lake, Freshwater Biology, 39, 1794, https://doi.org/10.1111/j.1365-2427.2010.02408.x, 2010.

Biester, H., Knorr, K.-H., Schellekens, J., Basler, A., and Hermanns, Y.-M.: Comparison of different methods to determine the degree of peat decomposition in peat bogs, Biogeosciences, 11, 2691–2707, https://doi.org/10.5194/bg-11-2691-2014, 2014.

Blodau, C.: Thermodynamic Control on Terminal Electron Transfer and Methanogenesis, in: Aquatic Redox Chemistry, edited by: Tratnyek, P. G., Grundl, T. J., and Haderlein, S. B., American Chemical Society, Washington, DC, 65–83, https://doi.org/10.1021/bk-2011-1071.ch004, 2011.

Blodau, C., Siems, M., and Beer, J.: Experimental burial inhibits methanogenesis and anaerobic decomposition in water-saturated peats, Environmental science & technology, 45, 9984–9989, https://doi.org/10.1021/es201777u, 2011.

Bonaiuti, S., Blodau, C., and Knorr, K.-H.: Transport, anoxia and end-product accumulation control carbon dioxide and methane production and release in peat soils, Biogeochemistry, 133, 219–239, https://doi.org/10.1007/s10533-017-0328-7, 2017.

Boudreau, B. P., Algar, C., Johnson, B. D., Croudace, I., Reed, A., Furukawa, Y., Dorgan, K. M., Jumars, P. A., Grader, A. S., and Gardiner, B. S.: Bubble growth and rise in soft sediments, Geol, 33, 517, https://doi.org/10.1130/G21259.1, 2005.

Broder, T., Blodau, C., Biester, H., and Knorr, K. H.: Peat decomposition records in three pristine ombrotrophic bogs in southern Patagonia, Biogeosciences, 9, 1479–1491, https://doi.org/10.5194/bg-9-1479-2012, 2012.

Burdige, D. J.: Preservation of organic matter in marine sediments: Controls, mechanisms, and an imbalance in sediment organic carbon budgets?, Chemical reviews, 107, 467–485, https://doi.org/10.1021/cr050347q, 2007.

Cocozza, C., D'Orazio, V., Miano, T. M., and Shotyk, W.: Characterization of solid and aqueous phases of a peat bog profile using molecular fluorescence spectroscopy, ESR and FT-IR, and comparison with physical properties, Organic Geochemistry, 34, 49–60, https://doi.org/10.1016/S0146-6380(02)00208-5, 2003.

https://doi.org/10.5194/bg-2019-284
Preprint. Discussion started: 29 August 2019

Cole, J. J., Prairie, Y. T., Caraco, N. F., McDowell, W. H., Tranvik, L. J., Striegl, R. G., Duarte, C. M., Kortelainen, P., Downing, J. A., Middelburg, J. J., and Melack, J.: Plumbing the Global Carbon Cycle: Integrating Inland Waters into the Terrestrial Carbon Budget, Ecosystems, 10, 172–185, https://doi.org/10.1007/s10021-006-9013-8, 2007.

Conrad, R.: Contribution of hydrogen to methane production and control of hydrogen concentrations in methanogenic soils and sediments, FEMS Microbiology Ecology, 28, 193–202, https://doi.org/10.1016/S0168-6496(98)00086-5, 1999.

Conrad, R., Noll, M., Claus, P., Klose, M., Bastos, W. R., and Enrich-Prast, A.: Stable carbon isotope discrimination and microbiology of methane formation in tropical anoxic lake sediments, Biogeosciences, 8, 795–814, https://doi.org/10.5194/bg-8-795-2011, 2011.

den Heyer, C. and Kalff, J.: Organic matter mineralization rates in sediments: A within- and among-lake study, Limnol. Oceanogr., 43, 695–705, https://doi.org/10.4319/lo.1998.43.4.0695, 1998.

Deutscher Wetterdienst (DWD): Observations Germany - Climate - Multi-annual mean 81-10, ftp://ftp-cdc.dwd.de/pub/CDC/observations_germany/climate/multi_annual/mean_81-10/, last access: 21 May 2019, 2019.

Dinno, A.: dunn.test: Dunn's Test of Multiple Comparisons Using Rank Sums, 2017.

Downing, J. A.: Emerging global role of small lakes and ponds: little things mean a lot, Limnetica, 29, 9–23, 2010.

Downing, J. A., Prairie, Y. T., Cole, J. J., Duarte, C. M., Tranvik, L. J., Striegl, R. G., McDowell, W. H., Kortelainen, P., Caraco, N. F., Melack, J. M., and Middelburg, J. J.: The global abundance and size distribution of lakes, ponds, and impoundments, Limnol. Oceanogr., 51, 2388–2397, https://doi.org/10.4319/lo.2006.51.5.2388, 2006.

Duc, N. T., Crill, P., and Bastviken, D.: Implications of temperature and sediment characteristics on methane formation and oxidation in lake sediments, Biogeochemistry, 100, 185–196, https://doi.org/10.1007/s10533-010-9415-8, 2010.

Ellenberg, H., Weber, H. E., Düll, R., Wirth, V., and Werner, W.: Zeigerwerte von Pflanzen in Mitteleuropa, 3., durchgesehene Auflage, Scripta geobotanica, Volume 18, Verlag Erich Goltze GmbH & Co KG, Göttingen, 262 pp., 2001.

Falz, K. Z., Holliger, C., Großkopf, R., Liesack, W., Nozhevnikova, A. N., Müller, B., Wehrli, B., and Hahn, D.: Vertical Distribution of Methanogens in the Anoxic Sediment of Rotsee (Switzerland), Applied and Environmental Microbiology, 65, 2402–2408, 1999.

Fenchel, T., King, G. M., and Blackburn, T. H.: Bacterial biogeochemistry: The ecophysiology of mineral cycling, 3rd ed., Academic Press/Elsevier, Boston, Mass, 2012.

Fey, A. and Conrad, R.: Effect of temperature on the rate limiting step in the methanogenic degradation pathway in rice field soil, Soil Biology and Biochemistry, 35, 1–8, https://doi.org/10.1016/S0038-0717(02)00175-X, 2003.

Fox, J. and Weisberg, S.: An {R} Companion to Applied Regression, Sage, Thousand Oaks, CA, 2011.

https://doi.org/10.5194/bg-2019-284
Preprint. Discussion started: 29 August 2019

Biogeosciences
Discussions

Fuchs, A., Lyautey, E., Montuelle, B., and Casper, P.: Effects of increasing temperatures on methane concentrations and methanogenesis during experimental incubation of sediments from oligotrophic and mesotrophic lakes, J. Geophys. Res. Biogeosci., 121, 1394–1406, https://doi.org/10.1002/2016JG003328, 2016.

Gao, C., Sander, M., Agethen, S., and Knorr, K.-H.: Electron accepting capacity of dissolved and particulate organic matter control CO_2 and CH_4 formation in peat soils, Geochimica et Cosmochimica Acta, 245, 266–277, https://doi.org/10.1016/j.gca.2018.11.004, 2019.

Gilboa-Garber, N.: Direct spectrophotometric determination of inorganic sulfide in biological materials and in other complex mixtures, Analytical Biochemistry, 43, 129–133, https://doi.org/10.1016/0003-2697(71)90116-3, 1971.

Grasset, C., Mendonça, R., Villamor Saucedo, G., Bastviken, D., Roland, F., and Sobek, S.: Large but variable methane production in anoxic freshwater sediment upon addition of allochthonous and autochthonous organic matter, Limnol. Oceanogr., 63, 1488–1501, https://doi.org/10.1002/lno.10786, 2018.

Gudasz, C., Sobek, S., Bastviken, D., Koehler, B., and Tranvik, L. J.: Temperature sensitivity of organic carbon mineralization in contrasting lake sediments, J. Geophys. Res. Biogeosci., 120, 1215–1225, https://doi.org/10.1002/2015JG002928, 2015.

Gudasz, C., Bastviken, D., Steger, K., Premke, K., Sobek, S., and Tranvik, L. J.: Temperature-controlled organic carbon mineralization in lake sediments, Nature, 466, 478–481, https://doi.org/10.1038/nature09186, 2010.

Hoehler, T. M., Alperin, M. J., Albert, D. B., and Martens, C. S.: Apparent minimum free energy requirements for methanogenic Archaea and sulfate-reducing bacteria in an anoxic marine sediment, FEMS Microbiology Ecology, 38, 33–41, https://doi.org/10.1111/j.1574-6941.2001.tb00879.x, 2001.

Holgerson, M. A. and Raymond, P. A.: Large contribution to inland water CO_2 and CH_4 emissions from very small ponds, Nature Geosci, 9, 222–226, https://doi.org/10.1038/NGEO2654, 2016.

Hornibrook, E. R.C., Longstaffe, F. J., and Fyfe, W. S.: Spatial distribution of microbial methane production pathways in temperate zone wetland soils: Stable carbon and hydrogen isotope evidence, Geochimica et Cosmochimica Acta, 61, 745–753, https://doi.org/10.1016/S0016-7037(96)00368-7, 1997.

Jankowski, T., Livingstone, D. M., Bührer, H., Forster, R., and Niederhauser, P.: Consequences of the 2003 European heat wave for lake temperature profiles, thermal stability, and hypolimnetic oxygen depletion: Implications for a warmer world, Limnol. Oceanogr., 51, 815–819, https://doi.org/10.4319/lo.2006.51.2.0815, 2006.

Kammann, C., Grünhage, L., and Jäger, H.-J.: A new sampling technique to monitor concentrations of CH_4 N_2O and CO_2 in air at well-defined depths in soils with varied water potential, European Journal of Soil Science, 52, 297–303, https://doi.org/10.1046/j.1365-2389.2001.00380.x, 2001.

https://doi.org/10.5194/bg-2019-284
Preprint. Discussion started: 29 August 2019

Biogeosciences Discussions

Kampf, J.: Grundwasserlandschaften: Hydrologischer Atlas Rheinland-Pfalz, Landesamt für Umwelt, Wasserwirtschaft und Gewerbeaufsicht Rheinland-Pfalz, Mainz, 2005.

Kappes, H. and Sinsch, U.: Tolerance of Ceriodaphnia quadrangula and Diaphanosoma brachyurum (Crustacea: Cladocera) to experimental soft water acidification, Hydrobiologia, 109–115, 2005.

Kappes, H., Mechenich, C., and Sinsch, U.: Long-term dynamics of Asplanchna priodonta in Lake Windsborn with comments on the diet, Hydrobiologia, 432, 91–100, https://doi.org/10.1023/A:1004022020346, 2000.

Kiuru, P., Ojala, A., Mammarella, I., Heiskanen, J., Kämäräinen, M., Vesala, T., and Huttula, T.: Effects of Climate Change on CO_2 Concentration and Efflux in a Humic Boreal Lake: A Modeling Study, J. Geophys. Res. Biogeosci., 123, 2212–2233, https://doi.org/10.1029/2018JG004585, 2018.

Kling, G. W., Kipphut, G. W., and Miller, M. C.: The flux of CO_2 and CH_4 from lakes and rivers in arctic Alaska, Hydrobiologia, 240, 23–36, https://doi.org/10.1007/BF00013449, 1992.

Klüpfel, L., Piepenbrock, A., Kappler, A., and Sander, M.: Humic substances as fully regenerable electron acceptors in recurrently anoxic environments, Nature Geosci, 7, 195–200, https://doi.org/10.1038/NGEO2084, 2014.

Konhauser, K.: Introduction to geomicrobiology, John Wiley & Sons Ltd, Hoboken, 425 pp., 2009.

Kuhry, P. and Vitt, D. H.: Fossil Carbon/Nitrogen Ratios as a Measure of Peat Decomposition, Ecology, 77, 271–275, https://doi.org/10.2307/2265676, 1996.

Landesamt für Umwelt (LfU): Seenatlas: Windsborn Kratersee, https://geodaten-wasser.rlp-umwelt.de/prj-wwvauskunft/projects/seenatlas/daten/register1.jsp?seeId=125&see_bez=Windsborn+Kratersee&showHydrologie=true&showChemismus=true, last access 17 July 2019, 2013.

Lau, M. P., Sander, M., Gelbrecht, J., and Hupfer, M.: Spatiotemporal redox dynamics in a freshwater lake sediment under alternating oxygen availabilities: Combined analyses of dissolved and particulate electron acceptors, Environ. Chem., 13, 826, https://doi.org/10.1071/EN15217, 2016.

Lau, M. P., Sander, M., Gelbrecht, J., and Hupfer, M.: Solid phases as important electron acceptors in freshwater organic sediments, Biogeochemistry, 123, 49–61, https://doi.org/10.1007/s10533-014-0052-5, 2015.

Li, Y., Zhang, H., Tu, C., Fu, C., Xue, Y., and Luo, Y.: Sources and fate of organic carbon and nitrogen from land to ocean: Identified by coupling stable isotopes with C/N ratio, Estuarine, Coastal and Shelf Science, 181, 114–122, https://doi.org/10.1016/j.ecss.2016.08.024, 2016.

Liikanen, A., Murtoniemi, T., Tanskanen, H., Väisänen, T., and Martikainen, P. J.: Effects of temperature and oxygen availability on greenhouse gas and nutrient dynamics in sediment of a eutrophic and mid-boreal lake, Biogeochemistry, 59, 269–286, https://doi.org/10.1023/A:1016015526712, 2002.

https://doi.org/10.5194/bg-2019-284
Preprint. Discussion started: 29 August 2019

Liu, L., Wilkinson, J., Koca, K., Buchmann, C., and Lorke, A.: The role of sediment structure in gas bubble storage and release, J. Geophys. Res. Biogeosci., 121, 1992–2005, https://doi.org/10.1002/2016JG003456, 2016.

Liu, L., Kock, T. de, Wilkinson, J., Cnudde, V., Xiao, S., Buchmann, C., Uteau, D., Peth, S., and Lorke, A.: Methane Bubble Growth and Migration in Aquatic Sediments Observed by X-ray µCT, Environ. Sci. Technol., 52, 2007–2015, https://doi.org/10.1021/acs.est.7b06061, 2018.

Lojen, S., Ogrinc, N., and Dolenec, T.: Decomposition of sedimentary organic matter and methane formation in the recent sediment of Lake Bled (Slovenia), Chemical Geology, 159, 223–240, https://doi.org/10.1016/S0009-2541(99)00032-7, 1999.

Lovley, D. R., Coates, J. D., Blunt-Harris, E. L., Phillips, E. J. P., and Woodward, J. C.: Humic substances as electron acceptors for microbial respiration, Nature, 382, 445–448, https://doi.org/10.1038/382445a0, 1996.

Malmer, N. and Holm, E.: Variation in the C/N-Quotient of Peat in Relation to Decomposition Rate and Age Determination with 210 Pb, Oikos, 43, 171, https://doi.org/10.2307/3544766, 1984.

McLatchey, G. P. and Reddy, K. R.: Regulation of Organic Matter Decomposition and Nutrient Release in a Wetland Soil, Journal of Environment Quality, 27, 1268, https://doi.org/10.2134/jeq1998.00472425002700050036x, 1998.

Megonigal, J. P., Hines, M. E., and Visscher, P. T.: Anaerobic Metabolism: Linkages to Trace Gases and Aerobic Processes, in: Treatise on Geochemistry, Elsevier, 317–424, https://doi.org/10.1016/B0-08-043751-6/08132-9, 2003.

Meyer, W.: Geologie der Eifel, 4th ed., Schweizerbart'sche Verlagsbuchhandlung, Stuttgart, 2013.

Meyers, P. A.: Preservation of elemental and isotopic source identification of sedimentary organic matter, Chemical Geology, 114, 289–302, https://doi.org/10.1016/0009-2541(94)90059-0, 1994.

Miyajima, T., Wada, E., Hanba, Y. T., and Vijarnsorn, P.: Anaerobic mineralization of indigenous organic matters and methanogenesis in tropical wetland soils, Geochimica et Cosmochimica Acta, 61, 3739–3751, https://doi.org/10.1016/S0016-7037(97)00189-0, 1997.

Muri, G. and Wakeham, S. G.: Organic matter and lipids in sediments of Lake Bled (NW Slovenia): Source and effect of anoxic and oxic depositional regimes, Organic Geochemistry, 37, 1664–1679, https://doi.org/10.1016/j.orggeochem.2006.07.016, 2006.

Natchimuthu, S., Sundgren, I., Gålfalk, M., Klemedtsson, L., and Bastviken, D.: Spatiotemporal variability of lake pCO_2 and CO_2 fluxes in a hemiboreal catchment, J. Geophys. Res. Biogeosci., 122, 30–49, https://doi.org/10.1002/2016JG003449, 2017.

Natchimuthu, S., Sundgren, I., Gålfalk, M., Klemedtsson, L., Crill, P., Danielsson, Å., and Bastviken, D.: Spatio-temporal variability of lake CH_4 fluxes and its influence on annual whole lake emission estimates, Limnol. Oceanogr., 61, S13-S26, https://doi.org/10.1002/lno.10222, 2016.

Niemeyer, J., Chen, Y., and Bollag, J.-M.: Characterization of Humic Acids, Composts, and Peat by Diffuse Reflectance Fourier-Transform Infrared Spectroscopy, Soil Science Society of America Journal, 56, 135, https://doi.org/10.2136/sssaj1992.03615995005600010021x, 1992.

OENorm B 4412: 1974 07 01, Erd- und Grundbau; Untersuchung von Bodenproben; Korngrößenverteilung, 1974.

OENorm L 1050: 2016 03 15, Boden als Pflanzenstandort - Begriffe und Untersuchungsverfahren, 2016.

OENorm L 1061-2: 2019 03 01, Physikalische Bodenuntersuchungen - Bestimmung der Korngrößenverteilung des Mineralbodens in land- und forstwirtschaftlich genutzten Böden - Teil 2: Feinboden, 2019.

Ostrovsky, I. and Tęgowski, J.: Hydroacoustic analysis of spatial and temporal variability of bottom sediment characteristics in Lake Kinneret in relation to water level fluctuation, Geo-Mar Lett, 30, 261–269, https://doi.org/10.1007/s00367-009-0180-4, 2010.

R Core Team: R: A language and environment for statistical computing, R Foundation for Statistical Computing, Vienna, Austria, 2018.

Raymond, P. A., Hartmann, J., Lauerwald, R., Sobek, S., McDonald, C., Hoover, M., Butman, D., Striegl, R., Mayorga, E., Humborg, C., KORTELAINEN, P., Dürr, H., Meybeck, M., Ciais, P., and Guth, P.: Global carbon dioxide emissions from inland waters, Nature, 503, 355–359, https://doi.org/10.1038/nature12760, 2013.

Regnier, P., Friedlingstein, P., Ciais, P., Mackenzie, F. T., Gruber, N., Janssens, I. A., Laruelle, G. G., Lauerwald, R., Luyssaert, S., Andersson, A. J., Arndt, S., Arnosti, C., Borges, A. V., Dale, A. W., Gallego-Sala, A., Goddéris, Y., Goossens, N., Hartmann, J., Heinze, C., Ilyina, T., Joos, F., LaRowe, D. E., Leifeld, J., Meysman, F. J. R., Munhoven, G., Raymond, P. A., Spahni, R., Suntharalingam, P., and Thullner, M.: Anthropogenic perturbation of the carbon fluxes from land to ocean, Nature Geosci, 6, 597–607, https://doi.org/10.1038/NGEO1830, 2013.

Romeijn, P., Comer-Warner, S. A., Ullah, S., Hannah, D. M., and Krause, S.: Streambed Organic Matter Controls on Carbon Dioxide and Methane Emissions from Streams, Environ. Sci. Technol., 53, 2364–2374, https://doi.org/10.1021/acs.est.8b04243, 2019.

Sander, R.: Compilation of Henry's law constants (version 4.0) for water as solvent, Atmos. Chem. Phys., 15, 4399–4981, https://doi.org/10.5194/acp-15-4399-2015, 2015.

Schilder, J., Bastviken, D., van Hardenbroek, M., Kankaala, P., Rinta, P., Stötter, T., and Heiri, O.: Spatial heterogeneity and lake morphology affect diffusive greenhouse gas emission estimates of lakes, Geophys. Res. Lett., 40, 5752–5756, https://doi.org/10.1002/2013GL057669, 2013.

Schink, B.: Energetics of syntrophic cooperation in methanogenic degradation, Microbiology and molecular biology reviews MMBR, 61, 262–280, 1997.

Schoell, M.: Multiple origins of methane in the Earth, Chemical Geology, 71, 1–10, https://doi.org/10.1016/0009-2541(88)90101-5, 1988.

https://doi.org/10.5194/bg-2019-284
Preprint. Discussion started: 29 August 2019

Schwarz, J. I. K., Eckert, W., and Conrad, R.: Response of the methanogenic microbial community of a profundal lake sediment (Lake Kinneret, Israel) to algal deposition, Limnol. Oceanogr., 53, 113–121, https://doi.org/10.4319/lo.2008.53.1.0113, 2008.

Seeberg-Elverfeldt, J., Schlüter, M., Feseker, T., and Kölling, M.: Rhizon sampling of porewaters near the sediment-water interface of aquatic systems, Limnol. Oceanogr. Methods, 3, 361–371, https://doi.org/10.4319/lom.2005.3.361, 2005.

Segers, R.: Methane production and methane consumption: a review of processes underlying wetland methane fluxes, Biogeochemistry, 41, 23–51, https://doi.org/10.1023/A:1005929032764, 1998.

Sobek, S., Durisch-Kaiser, E., Zurbrügg, R., Wongfun, N., Wessels, M., Pasche, N., and Wehrli, B.: Organic carbon burial efficiency in lake sediments controlled by oxygen exposure time and sediment source, Limnol. Oceanogr., 54, 2243–2254, https://doi.org/10.4319/lo.2009.54.6.2243, 2009.

Spafford, L. and Risk, D.: Spatiotemporal Variability in Lake-Atmosphere Net CO 2 Exchange in the Littoral Zone of an Oligotrophic Lake, J. Geophys. Res. Biogeosci., 123, 1260–1276, https://doi.org/10.1002/2017JG004115, 2018.

Stumm, W. and Morgan, J. J.: Aquatic chemistry: Chemical equilibria and rates in natural waters, Third edition, A Wiley-Interscience publication, John Wiley & Sons Inc, New York, Chichester, Brisbane, Toronto, Singapore, 1022 pp., 1996.

Tamura, H., Goto, K., Yotsuyanagi, T., and Nagayama, M.: Spectrophotometric determination of iron(II) with 1,10-phenanthroline in the presence of large amounts of iron(III), Talanta, 21, 314–318, 1974.

Tfaily, M. M., Cooper, W. T., Kostka, J. E., Chanton, P. R., Schadt, C. W., Hanson, P. J., Iversen, C. M., and Chanton, J. P.: Organic matter transformation in the peat column at Marcell Experimental Forest: Humification and vertical stratification, J. Geophys. Res. Biogeosci., 119, 661–675, https://doi.org/10.1002/2013JG002492, 2014.

Tolu, J., Rydberg, J., Meyer-Jacob, C., Gerber, L., and Bindler, R.: Spatial variability of organic matter molecular composition and elemental geochemistry in surface sediments of a small boreal Swedish lake, Biogeosciences, 14, 1773–1792, https://doi.org/10.5194/bg-14-1773-2017, 2017.

Torres, I. C., Inglett, K. S., and Reddy, K. R.: Heterotrophic microbial activity in lake sediments: Effects of organic electron donors, Biogeochemistry, 104, 165–181, https://doi.org/10.1007/s10533-010-9494-6, 2011.

Updegraff, K., Pastor, J., Bridgham, S. D., and Johnston, C. A.: Environmental and Substrate Controls over Carbon and Nitrogen Mineralization in Northern Wetlands, Ecological Applications, 5, 151–163, https://doi.org/10.2307/1942060, 1995.

Verpoorter, C., Kutser, T., Seekell, D. A., and Tranvik, L. J.: A global inventory of lakes based on high-resolution satellite imagery, Geophys. Res. Lett., 41, 6396–6402, https://doi.org/10.1002/2014GL060641, 2014.

Walpen, N., Getzinger, G. J., Schroth, M. H., and Sander, M.: Electron-Donating Phenolic and Electron-Accepting Quinone Moieties in Peat Dissolved Organic Matter: Quantities and Redox Transformations in the Context of Peat Biogeochemistry, Environ. Sci. Technol., 52, 5236–5245, https://doi.org/10.1021/acs.est.8b00594, 2018.

Walpen, N., Schroth, M. H., and Sander, M.: Quantification of Phenolic Antioxidant Moieties in Dissolved Organic Matter by Flow-Injection Analysis with Electrochemical Detection, Environ. Sci. Technol., 50, 6423–6432, https://doi.org/10.1021/acs.est.6b01120, 2016.

West, W. E., Coloso, J. J., and Jones, S. E.: Effects of algal and terrestrial carbon on methane production rates and methanogen community structure in a temperate lake sediment, Freshwater Biology, 57, 949–955, https://doi.org/10.1111/j.1365-2427.2012.02755.x, 2012.

Wetzel, R. G.: Gradient-dominated ecosystems: Sources and regulatory functions of dissolved organic matter in freshwater ecosystems, in: Dissolved Organic Matter in Lacustrine Ecosystems: Energy Source and System Regulator, edited by: Salonen, K., Kairesalo, T., and Jones, R. I., Springer Netherlands, Dordrecht, 181–198, https://doi.org/10.1007/978-94-011-2474-4_14, 1992.

Wetzel, R. G.: Gradient-dominated ecosystems: sources and regulatory functions of dissolved organic matter in freshwater ecosystems, in: Salonen K., Kairesalo T., Jones R.I. (eds) Dissolved Organic Matter in Lacustrine Ecosystems, 181–198.

Whiticar, M. J.: Carbon and hydrogen isotope systematics of bacterial formation and oxidation of methane, Chemical Geology, 161, 291–314, https://doi.org/10.1016/S0009-2541(99)00092-3, 1999.

Wik, M., Crill, P. M., Varner, R. K., and Bastviken, D.: Multiyear measurements of ebullitive methane flux from three subarctic lakes, J. Geophys. Res. Biogeosci., 118, 1307–1321, https://doi.org/10.1002/jgrg.20103, 2013.

Wilkinson, J., Maeck, A., Alshboul, Z., and Lorke, A.: Continuous Seasonal River Ebullition Measurements Linked to Sediment Methane Formation, Environ. Sci. Technol., 49, 13121–13129, https://doi.org/10.1021/acs.est.5b01525, 2015.

Yao, H., Conrad, R., Wassmann, R., and Neue, H. U.: Effect of soil characteristics on sequential reduction and methane production in sixteen rice paddy soils from China, the Philippines, and Italy, Biogeochemistry, 47, 269–295, https://doi.org/10.1007/BF00992910, 1999.